

Image Perception Wavelet Simulation and Enhancement  
for the Visually Impaired

THESIS  
Lemuel Ray Myers, Jr.  
Captain, USAF

AFIT/GEO/ENG/94D-03

This document has been approved  
for public release and sale; its  
distribution is unlimited

DEPARTMENT OF THE AIR FORCE  
AIR UNIVERSITY  
**AIR FORCE INSTITUTE OF TECHNOLOGY**

Wright-Patterson Air Force Base, Ohio

19941228 063

AFIT/GEO/ENG/94D-03

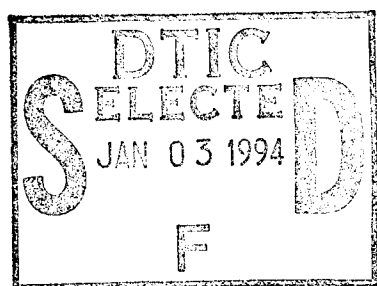


Image Perception Wavelet Simulation and Enhancement  
for the Visually Impaired

Accession For	
NTIS CRA&I	<input checked="" type="checkbox"/>
DTIC TAB	<input type="checkbox"/>
Unannounced	<input type="checkbox"/>
Justification	
By	
Dr. Burton /	
Approved by: Dr. Burton	
For	Approved and/or Supervised
A-1	

THESIS  
Lemuel Ray Myers, Jr.  
Captain, USAF

AFIT/GEO/ENG/94D-03

THIS IS AN UNCLASSIFIED DOCUMENT

Approved for public release; distribution unlimited

AFIT/GEO/ENG/94D-03

**Image Perception Wavelet Simulation and Enhancement for the Visually  
Impaired**

**THESIS**

**Presented to the Faculty of the School of Engineering  
of the Air Force Institute of Technology  
Air University  
In Partial Fulfillment of the  
Requirements for the Degree of  
Master of Science in Electrical Engineering**

**Lemuel Ray Myers, Jr., B.S.**

**Captain, USAF**

**December 1994**

**Approved for public release; distribution unlimited**

### *Acknowledgements*

I can't say thanks enough to my advisor, Dr. Steve Rogers, and his accomplice, Dr. Matt Kabrisky. Their verbal bludgeonings (and bantering) caused me to learn more than I ever thought possible. Thanks to Dr. Mark Cannon for putting up with my questions on human visual perception, to Dr. Eli Peli for perusing and commenting on my enhancement results, and to Dr. Greg Warhola and Dr. Tom Burns for patiently answering my wavelet questions.

Thanks to Bies, Kate, Terry and the whole Rogers gang for being there with help, advice, and humor.

Most of all, infinite thanks to Linda and Duncan; not only for their unwavering support and love, but also for their sacrifice during the last few months of preparing this document when I was at school more often than I was at home.

Lemuel Ray Myers, Jr.

## *Table of Contents*

	Page
Acknowledgements . . . . .	ii
List of Figures . . . . .	vi
List of Tables . . . . .	viii
Abstract . . . . .	ix
I. Introduction . . . . .	1
1.1 Background . . . . .	2
1.2 Problem Statement . . . . .	2
1.3 Research Questions . . . . .	3
1.4 Standards . . . . .	3
1.5 Scope . . . . .	3
1.6 Methodology . . . . .	4
1.7 Overview of Thesis . . . . .	4
II. Literature Review . . . . .	6
2.1 Introduction . . . . .	6
2.2 Human Visual System . . . . .	7
2.3 Artificial Viewing Environment . . . . .	9
2.4 Measurement of Contrast Sensitivity . . . . .	10
2.4.1 The staircase-method in psychophysics . . . . .	12
2.4.2 Parameter Estimation by Sequential Testing (PEST) . .	15
2.5 Measurement of Suprathreshold Characteristics . . . . .	17
2.6 Simulation of What a Person With a Given Threshold Curve Sees When Looking at an Image . . . . .	20

	Page
2.7 Digital Enhancement . . . . .	23
2.7.1 Contrast Manipulation . . . . .	24
2.7.2 Spatial Filtering . . . . .	25
2.7.3 Pseudocolor Recoding . . . . .	27
2.7.4 Compensation Filters . . . . .	27
2.7.5 Modified Pre-Emphasis Model . . . . .	29
2.8 Wavelets . . . . .	30
2.9 Headset . . . . .	39
2.10 Summary . . . . .	39
 III. Methodology . . . . .	41
3.1 Wavelets . . . . .	41
3.2 Wavelet Simulations . . . . .	44
3.3 Wavelet Enhancement . . . . .	47
3.4 Using Individual Suprathreshold Contrast Characteristics of a Patient for Enhancement . . . . .	49
3.5 Localization . . . . .	50
3.6 Metric of Enhancement Effect . . . . .	51
3.7 Summary . . . . .	53
 IV. Results . . . . .	54
4.1 Simulation of Macular Degeneration Using Wavelets . . . . .	54
4.2 Wavelet Enhancement . . . . .	57
4.3 Metric of Enhancement Effect . . . . .	57
4.4 Summary . . . . .	59
 V. Conclusions . . . . .	61
5.1 Analysis of Algorithms Reproduced . . . . .	61
5.2 Analysis of Original Algorithms . . . . .	61
5.3 Recommendations for Follow-On Research . . . . .	62

	Page
Appendix A. Peli Simulation . . . . .	64
Appendix B. Enhancement Algorithms . . . . .	66
Appendix C. Matlab Implementation of Biorthogonal Wavelets . . . . .	67
C.1 Coefficients . . . . .	67
C.2 Decomposition . . . . .	68
C.3 Reconstruction . . . . .	71
Appendix D. Wavelet Simulation Code . . . . .	74
Bibliography . . . . .	81
Vita . . . . .	84

## *List of Figures*

Figure	Page
1. Human eye . . . . .	7
2. Relationship between macula lutea and fovea. . . . .	8
3. Structure of the retina . . . . .	8
4. Optical pathway . . . . .	9
5. Low Vision Enhancement System Headset . . . . .	10
6. Grating . . . . .	11
7. Boxed Grating . . . . .	12
8. Gaussian Modulated Grating . . . . .	13
9. Ideal staircase method . . . . .	14
10. Typical staircase method . . . . .	14
11. Double staircase method . . . . .	15
12. Random double staircase method . . . . .	16
13. Threshold curves . . . . .	18
14. Suprathreshold curves . . . . .	19
15. Original image . . . . .	20
16. Log-cosine filters . . . . .	21
17. Band-pass and low-pass images . . . . .	22
18. Simulation of low vision . . . . .	23
19. Simulation of normal vision . . . . .	23
20. Result of histogram equalization on a low contrast image. . . . .	24
21. Thresholding . . . . .	25
22. Adaptive image enhancement . . . . .	26
23. Compensation filter enhancement . . . . .	28
24. Compensation filter . . . . .	28
25. Pre-emphasis filter . . . . .	29

Figure		Page
26.	Pre-emphasis filter enhancement . . . . .	30
27.	Decomposition Scale and Wavelet Functions . . . . .	33
28.	Decomposition flow chart . . . . .	34
29.	Wavelet frequency responses . . . . .	35
30.	Decomposition relationships . . . . .	36
31.	Reconstruction Scale and Wavelet Functions . . . . .	37
32.	Reconstruction of an image after a single level of decomposition . . . . .	37
33.	Active matrix LCD used in headset. . . . .	39
34.	Peli filters . . . . .	42
35.	Wavelet filters . . . . .	42
36.	Mirror quad image . . . . .	43
37.	Third Level Decomposition Detail Coefficients . . . . .	44
38.	Third Level Decomposition Approximation Coefficients . . . . .	44
39.	Scale and Wavelet Functions Used in Wavelet Simulation . . . . .	45
40.	Generation of un-shifted detail coefficients. . . . .	46
41.	Shifting in the downsampling . . . . .	48
42.	Laplacian Mask . . . . .	52
43.	Edge-detected Original Image . . . . .	53
44.	Edge-detected Pre-emphasis Filtered Image . . . . .	53
45.	Wavelet simulation of low vision . . . . .	54
46.	Wavelet simulation of normal vision . . . . .	55
47.	Wavelet simulation with adaptive filtering . . . . .	55
48.	Wavelet simulation with compensation filtering . . . . .	56
49.	Wavelet simulation with pre-emphasis filtering . . . . .	56
50.	Wavelet Enhancement (Gain=5) . . . . .	57
51.	Wavelet Enhancement (Gain=2) . . . . .	58
52.	Summary of Various Enhancements . . . . .	60

*List of Tables*

Table		Page
1.	Decomposition Scaling Function . . . . .	32
2.	Decomposition Wavelet Function . . . . .	32
3.	Edge Detection Metric According to Peli Simulation . . . . .	58
4.	Edge Detection Metric According to Wavelet Simulation . . . . .	59

*Abstract*

This research delves into the area of image enhancement for the visually impaired. Binocular macular degeneration, a visual impairment, affects many Americans; since this condition could not be corrected with conventional glasses, the literature suggested using an enhancement system which used a pre-emphasis algorithm to enhance the input image for output to the observer. The work of Dr. Eli Peli, a pioneer in the field of image enhancement, is examined and reproduced. Since his work concentrated mainly on frequency analysis of images, the bulk of this research involves using discrete wavelet analysis to augment that work. A biorthogonal wavelet set is used to enhance images. That same wavelet set is used to provide a simulation of a person's perception of an image based upon that person's contrast sensitivity function. The wavelet enhancement follows Dr. Peli's method of enhancement using a modified pre-emphasis filter. The wavelet enhancement results are similar to that technique, with the most notable difference being that wavelet enhancements tend to accentuate the horizontal and vertical details of the image more than the spatial frequency concentric filter techniques outlined by Peli and others. The perception simulations use wavelet analysis and are based on the work accomplished by Peli concerning "local band-limited contrast," with the frequency analysis of that work giving way to a wavelet analysis; the results here are significantly different than those results seen in the Peli simulation. A method to enhance images based on suprathreshold characteristics of the observer is outlined. Methods in the past have concentrated on contrast threshold analysis, so the suprathreshold method of enhancement is the next logical step. A method for optimizing localized image enhancement is presented. This method has been used to increase the resolution for pilots viewing virtual environments and could take advantage of the existing retinal tracking hardware and software already in existence to better enhance images for the visually impaired.

# Image Perception Wavelet Simulation and Enhancement for the Visually Impaired

## *I. Introduction*

This research focused on enhancing images for persons suffering from binocular macular degeneration, or loss of vision in the foveal area of both eyes. The macula lutea contains the highest concentration of cones (nerve endings giving rise to color vision) on the retina; the fovea lies at the center of the macula lutea where the lens focuses incoming light, and a person's visual acuity is directly correlated to the condition of the cells in this area. Persons suffering from central scotoma (darkness in the center of the eye) due to cell damage can have difficulty reading text and recognizing faces. Different degrees of macular damage require different visual enhancement techniques so people with low vision due to central scotoma can regain some of their original visual ability.

Conventional glasses are most useful if a person's visual impairment is due to aberrations of the lens of the eye; therefore, if people suffering from central scotoma are to be helped, a different method of correction must be made available. Johns-Hopkins is currently testing a new device known as the Low Vision Enhancement System (LVES, pronounced Elvis) which consists of a pair of binocular cameras, a single magnifying camera, and two overlapping LCD screens to present a virtual, enhanced world to a low-vision patient in the hopes that computer digital enhancement may improve the patient's ability to recognize faces and read text.

The largest part of this thesis effort concentrated on helping the visually impaired with two new approaches, both using a biorthogonal wavelet set. First, the wavelet decomposition detail coefficients were manipulated based on a viewer's contrast sensitivity function in order to gain insight into what is actually perceived by a patient when viewing an image. The choice of wavelets as a human perception diagnostic tool followed from the work of Wang (35) in

which he modeled human auditory perception using a wavelet basis set. The premise that human corticle cells exhibit some of the characteristics of a wavelet processor is supported by the work of Jones and Palmer (13) concerning modelling of simple receptive fields in the cortex of cats. Second, the effects of boosting certain detail coefficients in a given image were explored in the hope that this manipulation could be beneficial to a low-vision viewer.

A new method using suprathreshold characteristics of a patient for enhancement was also outlined as was using only the information in an image in the area of interest to the observer for enhancement.

### *1.1 Background*

Image enhancement for the visually impaired has been studied since 1984 when Dr. Eli Peli (26) conjectured that digital techniques could be used to improve face recognition ability. His subsequent research explored ways to enhance facial images using digital image processing, and he used frequency analysis as his primary tool for image manipulation. Wavelets have been used extensively as a method of extracting information contained in images (4, 14, 17, 18, 29). Wavelet decompositions are analogous to (but should not be confused with) frequency filter analysis and their implementation during image processing parallels the analysis done by Peli concerning both image enhancement and human perception of images.

### *1.2 Problem Statement*

Investigate frequency and wavelet analysis in conjunction with tested individual perception parameters to simulate the view of an image to a person with macular degeneration and to enhance images to be presented to persons with low vision due to binocular macular degeneration.

### *1.3 Research Questions*

Does wavelet analysis lend itself to a better understanding of how people with visual defects perceive images? Can discrete wavelet analysis be used for effective image enhancement?

### *1.4 Standards*

Dr. Eli Peli pioneered the idea of using digital image processing to enhance images for viewers with visual defects (26). He conjectured these enhancements would allow low-vision viewers to more readily discriminate details about their visual environment, and that in turn would improve their ability to recognize faces. He also provided the concept of "band-limited contrast" which described the contrast in a given image locally and allowed experimenters to simulate what a person with measured visual parameters might observe when looking at an image. He observed the effects of various enhancement techniques (outlined in Chapter II) and initiated testing of two techniques (adaptive filtering and adaptive thresholding) on patients with low vision. He and others attempted to tune the image enhancement for a specific patient by using the contrast sensitivity function of that patient as the guide for enhancement. Their enhancements were applied to the entire image.

### *1.5 Scope*

This research first investigates and reproduces the simulation of image perception based on Frequency analysis presented by Peli (23, 19). With those simulations reproduced, the discrete wavelet transform is used in an analogous manner to simulate human perception. Images are enhanced using techniques established by Peli (26, 22, 20, 24, 21, 7) and Lawton (15) and then compared to images enhanced using discrete wavelet analysis to parallel the aforementioned work by direct manipulation of the decomposition detail coefficients rather than the manipulation of the spatial frequency spectrum. After analyzing this information, a method of enhancement based on measured suprathreshold characteristics of an observer is

suggested. Finally, recommendations are made on the use of a retinal tracking device now available for enhancement.

### *1.6 Methodology*

Since this thesis was the first at AFIT to be concerned with image enhancement for the visually impaired, the first step was to discover what work had been done in that area. A literature search revealed the bulk of the research belonged to Dr. Eli Peli of the Eye Research Institute. First, his visual degradation models simulating central scotoma (19) were reproduced. Second, with these human perception simulations duplicated, Peli's face enhancement techniques (26, 22, 20, 24, 21, 7) and Lawton's letter enhancement techniques (15) (as applied to faces) were reproduced. Third, using Peli's work as a foundation, a new model was developed using a biorthogonal wavelet set to simulate image perception of a person with a given contrast sensitivity function. Fourth, that same biorthogonal wavelet set was used to enhance images based on a given person's visual perception. Fifth, a method was devised to enhance an image using information based on not only measured contrast threshold characteristics of an observer (as was done in the past), but also on measured suprathreshold characteristics of the patient combined with the rms contrast of the image being enhanced. Sixth, a scheme for enhancing only the area where the patient is looking using a retinal tracking device is outlined. Wavelets have never been used in the context of benefiting persons suffering from low vision. The bulk of this research explored the value of wavelets as enhancement tools, and also the validity of using wavelet analysis to simulate a person's vision based on that person's measured contrast threshold perception characteristics.

### *1.7 Overview of Thesis*

Chapter 2 provides a background of digital image enhancement methods and results to date, as well as a review of practical application of wavelet analysis of images. Chapter 3 covers various methodologies used to enhance images and simulate visual perception. Chapter 4

discusses the results of these previous experiments. Chapter 5 presents concluding arguments and work which could be done to further the research in this area.

## *II. Literature Review*

### *2.1 Introduction*

In 1972, Stockham investigated some of the mechanics of how visual information is processed in humans (32). In that paper, he explored how the human visual system (HVS) processes visual information and pointed out that our view of the world is not the actual world, but instead a simulation seemingly designed to maximize the amount of useful information about the scene being viewed. Ginsburg's 1978 dissertation concentrated on explaining the HVS in terms of filtering characteristics alone (8). There, he conjectured that the HVS could be modelled as octave bandwidth spatial filters with varying orientations. If, in fact, the HVS does behave as a filter bank, then measurement of the frequency response of the system would be the natural first step in any subsequent analysis of human perception.

Jones and Palmer demonstrated that invasive types of measurements are feasible when analyzing cats (12), but invasive techniques are not usually possible with human subjects. Contrast sensitivity measurements describe the minimum contrasts necessary for a tested subject to perceive a set of given spatial frequencies. These measurements allow us (the experimenters) to non-invasively glimpse what may be perceived by another person. Since this Thesis concerns itself with image enhancement for low-vision patients suffering from binocular macular degeneration, knowledge about how these people perceive their environment could be used to make their world more recognizable. Although presenting the world through an electronic headset would not be the same as seeing with perfect eyes, Stockham already pointed out that natural human visual perception is in fact the output of a complex system which uses, at a minimum, compression and edge enhancement (32); therefore, added processing is not as unnatural as it may at first appear.

To set the stage for an explanation of this research, a simple overview of the human visual system is presented in the next section.

## 2.2 Human Visual System

A diagram of the human eye is shown in figure 1. Light enters through the cornea and

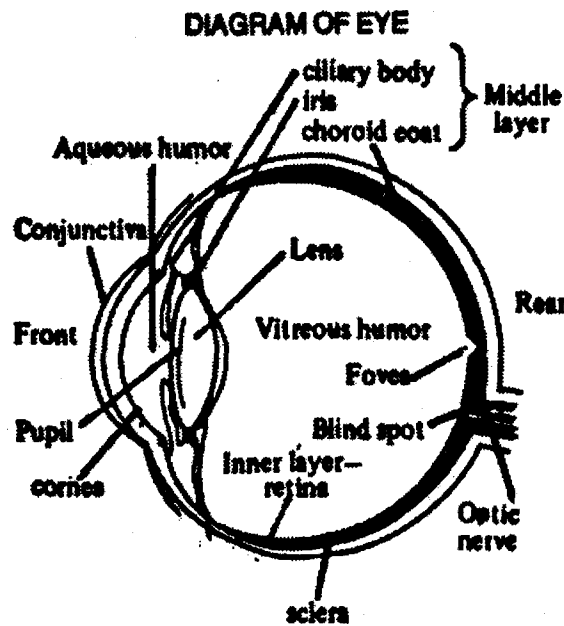


Figure 1. Human eye (30).

pupil, gets focused by the lens, traverses the vitreous humor, and finally strikes the retina. The area of the retina containing the highest concentration of cones is known as the macula lutea, at the center of which is a pit known as the fovea where the lens of the eye normally converges the incoming light. The relationship between the fovea and the macula lutea is shown in figure 2. The retina is composed of many layers of preprocessing cells, the last layer being the actual nerve endings. The multi-layer structure of the retina is shown in figure 3. Upon receiving the signal, the photo-receptor cells send the signal through the optic nerve to the area of the brain responsible for visual processing. The optical pathway is shown in figure 4.

This research concentrates on enhancing images so that they are more recognizable for people who have damage in the area of the macula lutea.

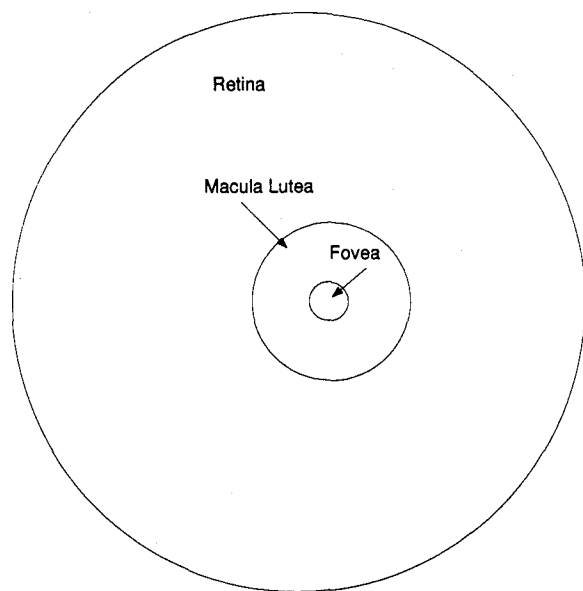


Figure 2. Relationship between macula lutea and fovea.

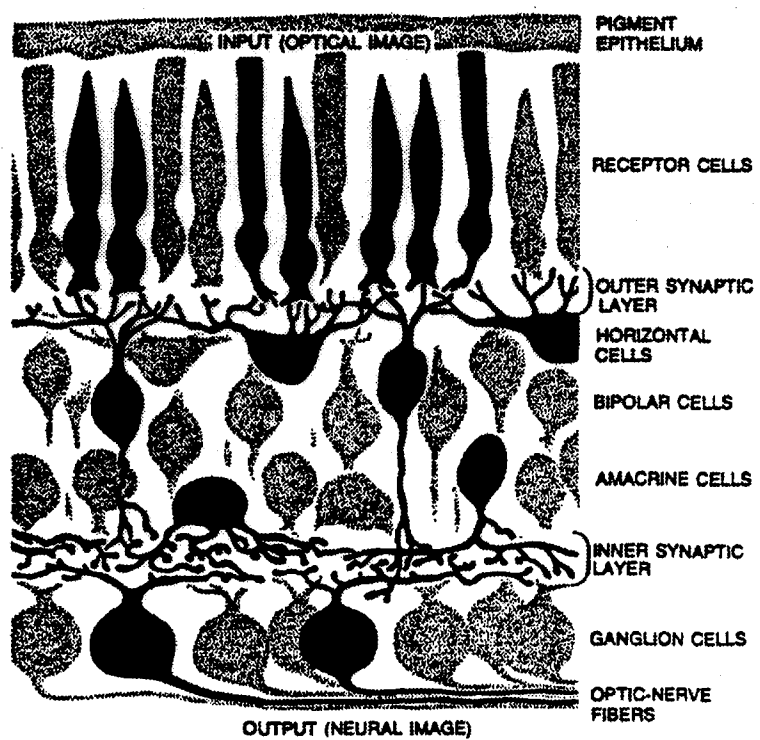


Figure 3. Structure of the retina(36).

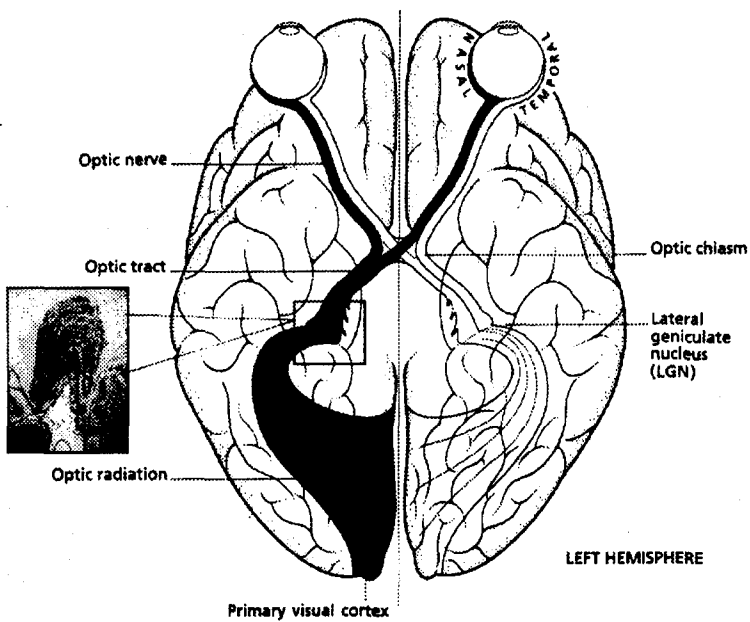


Figure 4. Optical pathway (39).

### 2.3 Artificial Viewing Environment

For any enhancement techniques to be practical in day-to-day applications of face recognition, a device must be employed which allows the user to have a clear view of the algorithm output. The obvious solution is for the subject to carry an enhancement system with at least three main components: an input camera, an enhancement computer, and an output screen or screens. One such device, the Low Vision Enhancement System (LVES, pronounced "Elvis") is currently being employed by Johns-Hopkins University. Figure 5 displays this device. It consists of three input cameras, two for binocular vision and one for magnification, and two miniature LCD output screens for the subject to view. Images are input by the cameras through an algorithm to be pre-processed in the hope that the subject will be able to more easily discern his environment.

In his 1992 paper concerning limitations of enhancement systems (21), Peli pointed out that since artificial displays have a finite dynamic range, if certain frequency components were amplified and then added back into the image these higher intensity values could exceed

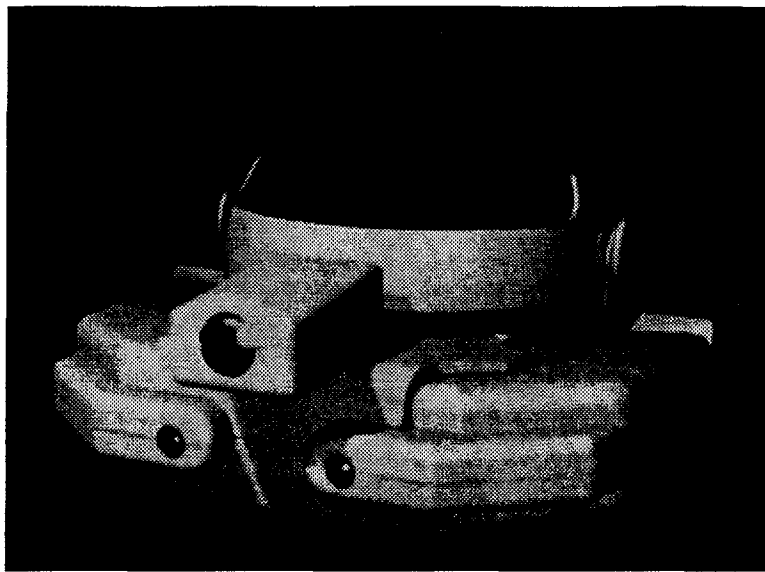


Figure 5. Low Vision Enhancement System (LVES) used as the input and output of an enhancement system.

the dynamic range of the display. This fact, perhaps considered a limitation, has been used to advantage in some of Peli's enhancement techniques. If the image was simply scaled to compensate, a signal amplitude loss occurred at all frequencies.

Also, if a display was utilized in a head-mounted device and robbed the patient of peripheral vision, vestibular problems could occur as a result of the magnification function associated with such a device (21). One solution to this could be to use a headset display that lay above the subject's normal field of view, one that could be referenced at will and would not block the subjects peripheral cues.

#### *2.4 Measurement of Contrast Sensitivity*

A subject's visual contrast threshold at a specific spatial frequency is the measure of the minimum contrast necessary for that subject to perceive a sinusoidal grating at that frequency. The contrast sensitivity curve is the inverse of this contrast threshold curve, and is a measure of how sensitive or receptive the subjects visual system is to a given frequency at threshold contrast.

Contrast in digital, gray-scale images is used to describe the relationships between pixel values in that image. The standard measure of contrast for a sinusoidal grating, an example of which is shown in figure 6, is

$$C = \frac{L_{max} - L_{min}}{L_{max} + L_{min}}, \quad 0 \leq C \leq 1 \quad (1)$$

where  $L_{max}$  is the maximum pixel value of the sinusoid and  $L_{min}$  is the minimum pixel value of the sinusoid, usually oscillating about some mean, DC level.

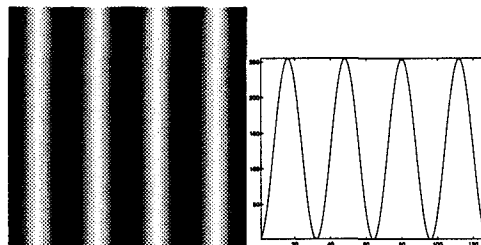


Figure 6. Left: sinusoidal grating with contrast  $C=1$ , Right: cross section of sinusoidal grating.

The Fourier spectrum of this stimulus was determined by three factors: the DC value of the stimulus (usually discarded by the experimenter since the area of interest was in the AC frequency spectrum), the frequency of the sinusoid (which transforms to a delta function at the frequency of interest), and the type of boundary surrounding the sinusoid (which determines what the frequency domain delta function will be convolved with). If a sinusoidal grating with frequency 8 cycles per image were surrounded by a background with intensity at the DC value of the grating, and the sinusoid's boundaries were formed by straight lines in the form of a box around the stimulus, the resulting frequency response would be as shown in figure 7. This indicates that the measurement of the response of the subject to this stimulus sheds light on the processing of the non-zero areas in the graph on the right in figure 7. To concentrate the area of interest more to the frequencies around 8 cycles per image, a sinusoid modulated by a two

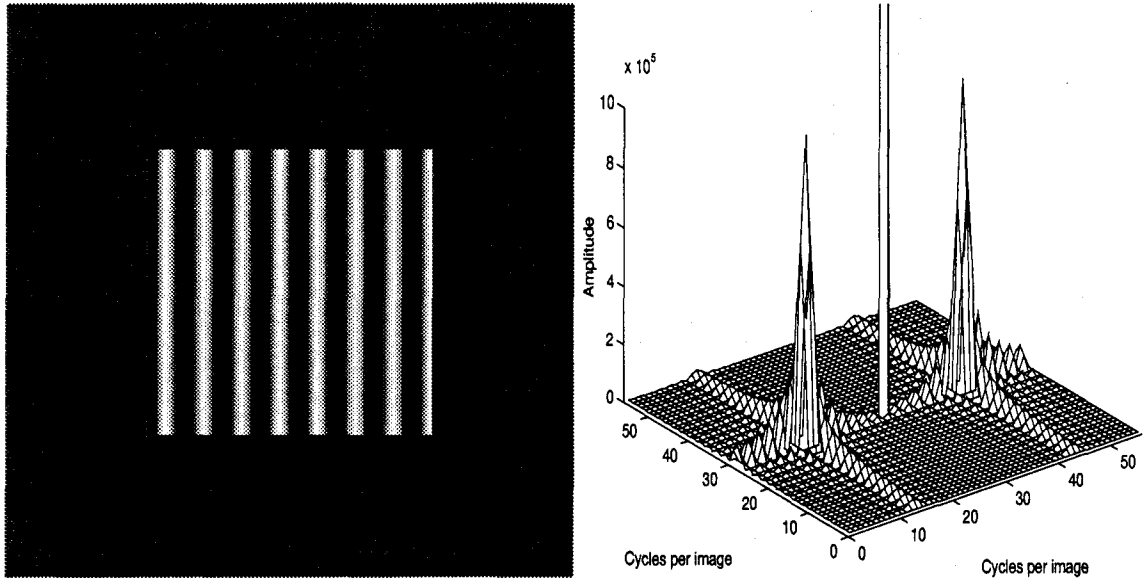


Figure 7. Left: boxed sinusoidal grating with contrast  $C=1$ . Right: closeup of frequency spectrum to include the area of interest, here 8 cycles per image.

dimensional Gaussian rather than a two dimensional rect function is sometimes used (25, 3). The result of this operation is shown in figure 8.

**2.4.1 The staircase-method in psychophysics.** When looking for a psychometric threshold, such as the minimum amplitude of a sinusoidal grating at a specific spatial frequency so that the grating is seen by a subject, Cornsweet argued that the staircase-method provides a powerful and efficient estimation tool (6). For the above example, a subject would be presented with a grating and respond with a positive or negative as to whether the stimulus was seen. If the answer was positive, the contrast of the sinusoid would be lowered; if the answer was negative, the contrast would be increased. In the ideal case, a subject's responses would simply oscillate about the threshold amplitude as shown in figure 9, and the threshold level would be estimated to lie between the points of the first reversal. Cornsweet points out that in actual experiments a subject's responses were not independent of one another and results obtained when trying to determine a visual threshold using the staircase method would more closely match those shown in figure 10. He said the actual threshold was usually estimated as

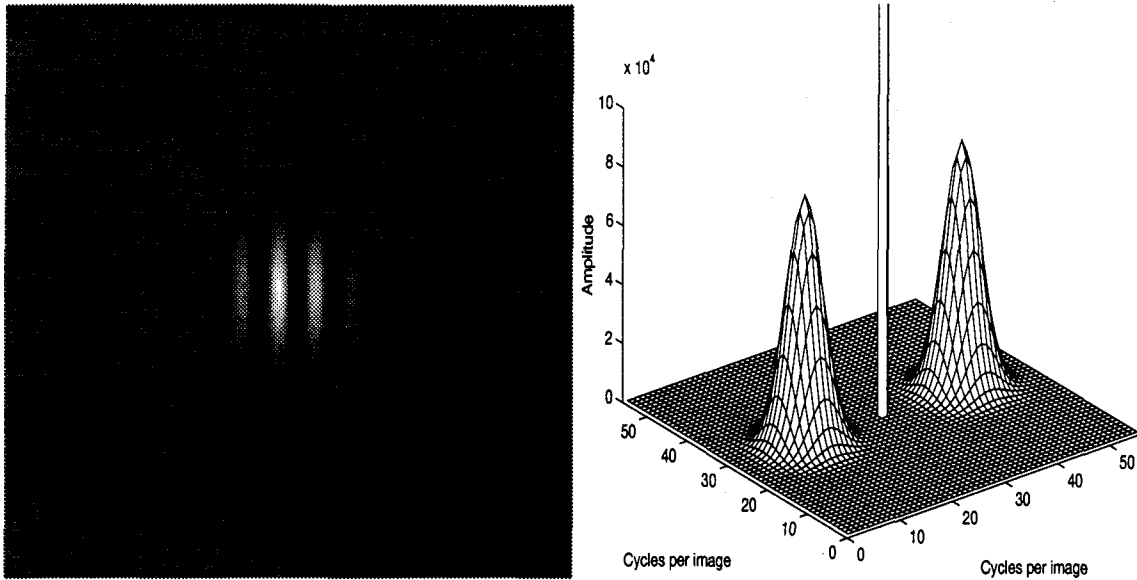


Figure 8. Left: sinusoidal grating with contrast  $C=1$  modulated by a two dimensional Gaussian function. Right: closeup of frequency spectrum to include the area of interest, once again 8 cycles per image.

the intensity level above which 50% of the responses were "yes" and below which 50% of the responses were "no".

The experimenter had control over four parameters when using the staircase-method: the initial amplitude or contrast, the step-sizes between subsequent trials, how many trials until the test was terminated, and modifications of step-size if warranted. The first few trials of a test such as this were necessary to establish the approximate range in which the threshold lay; therefore, the initial amplitude or contrast was chosen as closely as possible to the estimated threshold so that as few trials were made as necessary. The step-size between trials was ideally chosen to approximate sensory perception intervals that occur in nature. How many trials used depended on the experimenter's preference since a dichotomy existed between expediency (low number of trials) and accuracy (high number of trials). As the test progressed, the experimenter could alter step sizes in a heuristic fashion (see the next section concerning parameter estimation by sequential testing) to home in on the actual threshold being estimated.

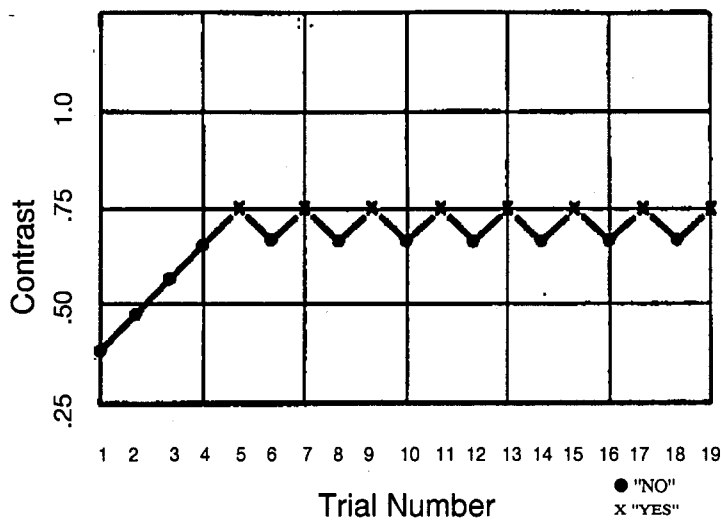


Figure 9. Ideal results of using the staircase-method to determine visual contrast threshold (6).

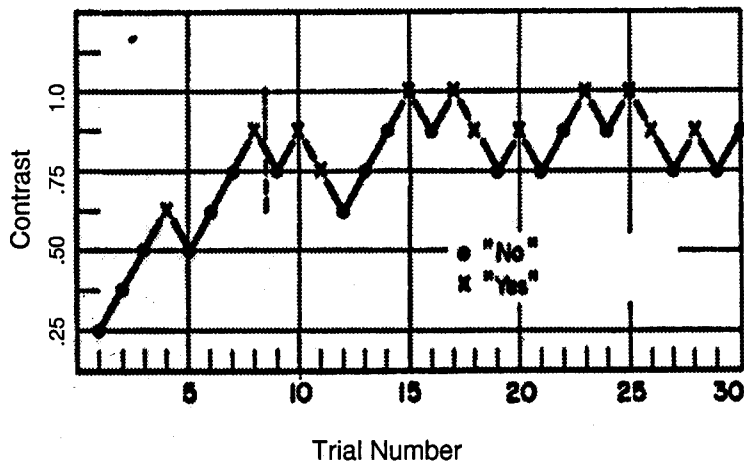


Figure 10. Typical results of using the staircase-method to determine visual contrast threshold (6).

One of the problems with this method as pointed out by Cornsweet was that if the answers at each trial consisted of a simple yes/no answer, a subject could essentially "close their eyes" as the testing proceeded and "game" the test (whether or not they realized they were doing it) so that the results would be unreliable. He conjectured that the double-staircase method offered a way to circumvent this problem. The first trial presented a testing level on one side of the estimated threshold while the second trial presented a testing level on the other side. See figure 11. Every other trial, then, belonged to a distinct set of two trials occurring simultaneously. To add another dimension, the test could randomly decide to which set a trial belonged as the test commenced as in figure 12. Cornsweet argued that the subject must then be responding to the actual stimuli and not guessing.

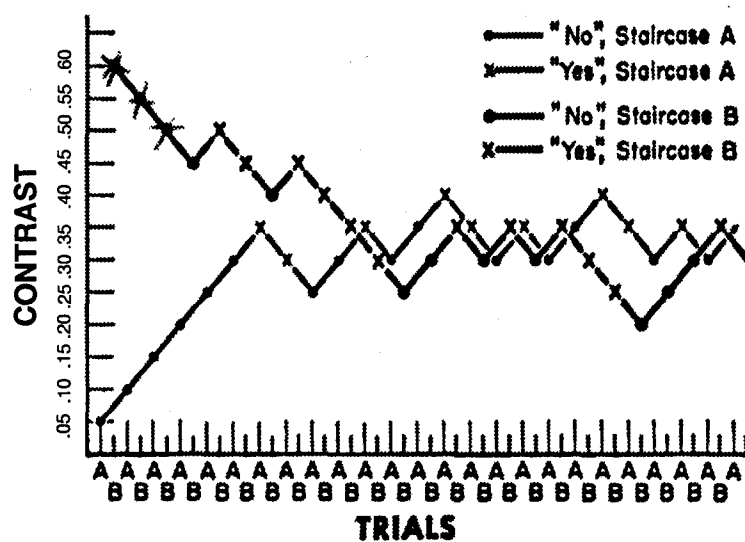


Figure 11. Possible results of using the double staircase method to determine threshold (6).

**2.4.2 Parameter Estimation by Sequential Testing (PEST).** Taylor expanded upon the staircase-method by providing a set of rules based on the Wald sequential likelihood-ratio test (34) as to when the testing level should be changed and the magnitude of that change (33). The PEST algorithm was to be an adaptive method of testing for a psychometric function in that the step size and number of trials would not depend exclusively on predetermined parameters, but would instead depend on previous trials in the same experiment. Taylor pointed out that

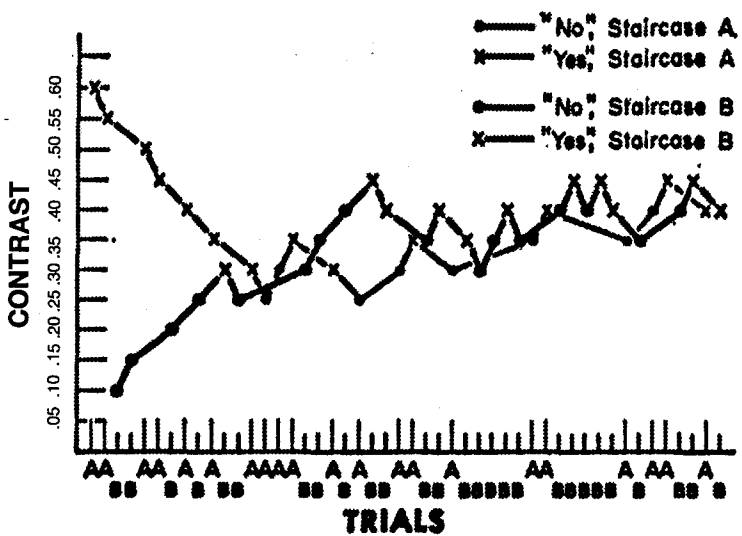


Figure 12. Possible results of using the random double staircase method to determine threshold (6).

the number of times to test at a current level was bounded by how many correct responses were expected at that level,

$$E[N(C)] = P_t \times T \pm W. \quad (2)$$

$N(C)$  was the total number of correct responses after each change in testing level,  $E[...]$  was the expected value operator, and  $W$  was a constant determined heuristically based on how powerful the test was to be. The deviation limit,  $W$ , determined the power versus speed dichotomy of the algorithm. Large  $W$  resulted in many trials and estimates very close to the actual threshold level, while small  $W$  caused rapid testing at the expense of accuracy.  $P_t$  was the target probability; this target probability was the ratio of the estimated number of correct responses to the number of trials at that particular testing level. For example, the experimenter could say he felt getting 5 out of 6 responses correct would indicate that the subject could, in fact, discriminate a horizontal grating from a vertical grating in a measure of contrast sensitivity. He would then set  $P_t = 5/6$  or .8333. The value chosen for  $P_t$  did not

effect the validity of the final estimate of the threshold level, but it did effect the number of trials necessary to arrive at that estimate.

In the context of testing for a contrast threshold curve for a given frequency, grating contrast of the next trial was based on preceding trials. Taylor's rules were outlined as follows:

- When the above boundary rule indicated a reversal of direction; for example, the contrast stopped going up and on the next step went down; the contrast step size was halved.
- When the boundary rule indicated the second step to be in the same direction as the first, the second step size was the same as the first.
- The size of the fourth, fifth, sixth, and so on, step in the same direction were double the preceding step size.
- The step size of the third successive step in the same direction depended on the last reversal preceding the current step direction series; if the step size preceding that reversal was double its preceding step, this step size was the same as the second step size; if the step size preceding that reversal was not double its preceding step, this step size was double the second step size.

The PEST terminated when a step was called for that equalled the experimenter's chosen minimum step size. The estimated value of the contrast threshold level being sought was then the next level called for after the last test. No testing occurred at that level. Methods have since been outlined by Pentland (28, 16) which minimize the number of trials necessary to obtain a given threshold measurement using PEST.

Peli generated contrast threshold curves for several subjects (19). These are shown in figure 13 and were generated using the PEST algorithm (33, 28) and sinusoidal Gabor patches (as shown in figure 8) at frequencies of 2, 4, 8, 16, and 32 cycles per image (cpi).

## 2.5 *Measurement of Suprathreshold Characteristics*

Cannon demonstrated that visual perception contrast curves generated by measuring contrast above threshold (suprathreshold) characteristics of an observer were not simply

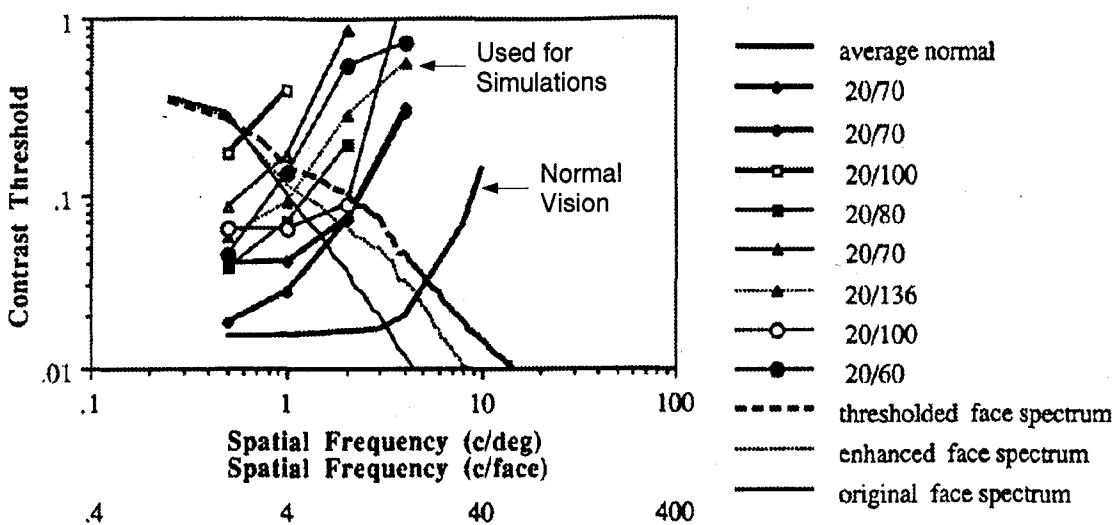


Figure 13. Various measured threshold curves of persons, the curve used for simulation purposes was the one corresponding to 20/136 vision (24)

contrast threshold curves shifted upward (2). He showed that as the overall contrast was increased for all spatial-frequency sinusoidal gratings, the amount of contrast necessary to make two spatial frequencies look as though they had the same contrast approached the same value. Figure 14 displays what these curves look like in normal individuals. For example; using one of the curves from figure 14, a sinusoidal grating varying at 4 cycles per deg (cpd) was displayed at a contrast of 0.010 and another grating varying at 16 cycles per deg was displayed simultaneously at some initial, different, contrast. The 16 cpd grating was adjusted by the subject until that subject perceived the two contrasts to be equal. On this particular curve, the actual contrast of the 16 cpd grating was around 0.020. The subject perceived the two contrasts to be equal even though the actual contrast of the 16 cpd grating was twice as high as the 4 cpd grating. At threshold, the subject perceived the 4 cpd grating at an actual threshold contrast and the 16 cpd grating at a different actual threshold contrast. As the 4 cpd grating contrast was increased, the perceptible difference between the 16 cpd actual contrast and the 4 cpd actual contrast *decreased*. This eventually led to a minimum contrast at which the actual contrasts of different spatial frequencies with the same contrast were perceived to be the same.

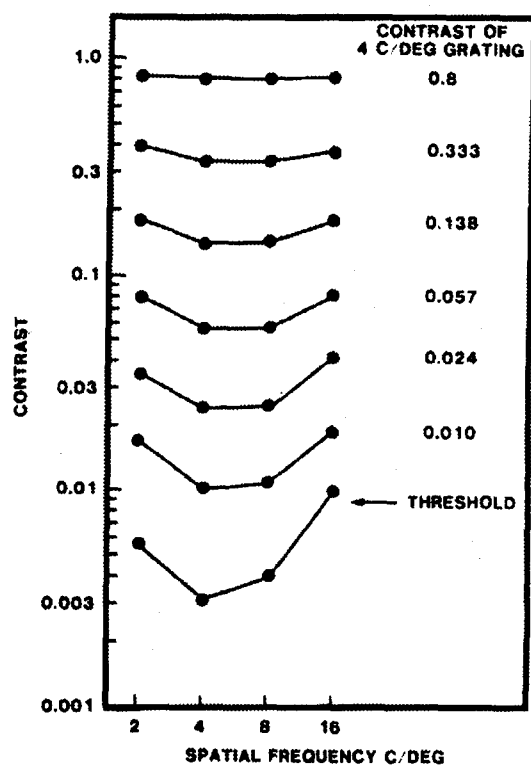


Figure 14. Example of suprathreshold curves in individuals with normal vision (2)

The method employed by Cannon to measure contrast suprathreshold characteristics of a subject was more straightforward than was the measurement of contrast threshold characteristics. The subject was presented a grating at a reference spatial frequency. Other spatial frequencies were presented and contrast matched by the subject to this reference frequency. The contrast of the reference frequency was increased for each set of tests until a flat curve was obtained.

## 2.6 *Simulation of What a Person With a Given Threshold Curve Sees When Looking at an Image*

To simulate how the human visual system processes information contained in an image, Peli proposed a nonlinear model using the concept of local band-limited contrast (19). This model generated a simulation of what a person with a given threshold curve saw when looking at an image. Figure 15 displays the 128x128 image presented to the observer in this example



Figure 15. Original Image (size 128 x 128)

simulation. The dimensions of the image in this figure are 1.257 inches square. If the reader holds the figure 1.5 feet from the eyes, the image subtends 4 degrees of arc; one cpd of the image is four cpi.

The first step in the simulation was to break the image into its constituent band-pass filtered components, much as Ginsburg conjectured the brain does (8). There were four images associated with each of the five spatial frequency contrast threshold responses obtained with the contrast sensitivity testing: four images associated with 2 cpi, four with 4 cpi, four with 8 cpi, four with 16 cpi, and four with 32 cpi. The first image generated was obtained by

filtering the original image's frequency spectrum with a concentric log-cosine filter of the form:

$$G_i(r) = 1/2[1 + \cos(\pi \log_2 r - \pi i)], i = 0, 1, 2, \dots \quad (3)$$

Plots of the band-pass filters centered at 2, 4, 8, 16, and 32 cpi are shown on the left in figure 16, and the related low-pass filters designed to capture the energy under their corresponding band-pass filter are shown on the right of that same figure. The text in the plot indicates where the center frequency of the band-pass filter lay and where the related low-pass filter became zero. Each band-pass filter was centered at  $2^i$  cpi and was one octave wide. Using 16 cpi as an

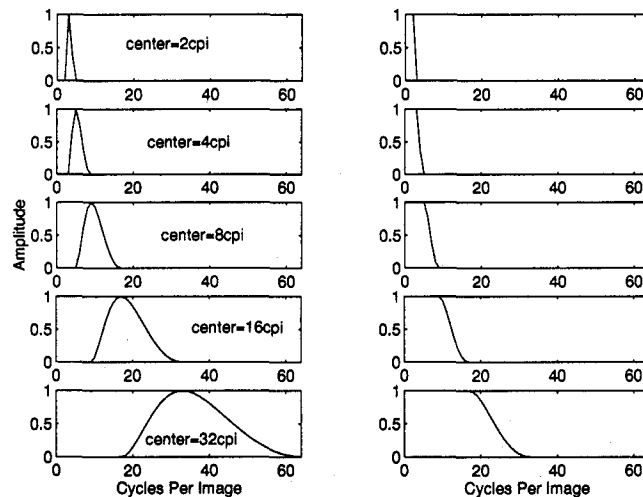


Figure 16. Cross-section log-cosine filters necessary for Peli's simulation.

example, the filter  $G_4$  was centered at 16 cpi and spanned from 8 to 32 cpi, with the amplitude of the filter at half maximum at frequencies of 12 and 24 cpi (thus, the octave bandwidth). For the simulation, the image generated by band pass filtering (center frequency 16 cpi) the original image is shown on the left in figure 17 and was point-by-point divided by the image

shown on the right in figure 17 which was generated by low-pass filtering the original image by the corresponding low-pass filter. The resulting image from this division was defined by



Figure 17. Left: image band-pass filtered with center of filter at 16 cycles per image (DC value of 128 added for image perception). Right: corresponding low-pass-filtered image.

Peli as a “local band-limited contrast image,” and each pixel value in each image was in fact a contrast in that band (in this case, 16 cpi) at that location. A local band-limited contrast image was generated for 2, 4, 8, 16, and 32 cycles per image. The pixel values, or contrasts, in each contrast image were compared to the threshold value measured in the contrast sensitivity test corresponding to the appropriate frequency. For example, if the contrast threshold of a subject at 16 cycles per image was .55, then each pixel value in the contrast image corresponding to 16 cycles per image, as in the above example, were compared to .55. If the pixel value was less than .55, the pixel value at that location in the image generated by the 16 cpi band-pass filter (left image in figure 17) was set to zero since the contrast at that location in that frequency band was below the observable threshold of the subject. If the pixel value was greater than or equal to .55, the value at that location in the bpf image was left alone. The images obtained by this process were called threshold images, and were added together along with the lowest frequency component to complete the simulation. Peli reasoned that this resulting image was representative of what a person with that particular threshold response would see when looking at figure 15. The threshold values used by Peli for his initial simulations were obtained from a subject with 20/136 vision shown on the graph in figure 13. Here, that same curve was used; the image produced is shown in figure 18 and represented what that low-vision observer perceived when looking at the original image. The Matlab code used to accomplish

this simulation is shown in Appendix A. To assure that the simulation was accurate for a person with normal vision, the curve representing normal vision in figure 13 was used in the simulation. The resulting picture was as shown in figure 19. Notice that while the high frequencies have been attenuated, the face is still recognizable (assuming, of course, that the reader has "normal" vision).



Figure 18. The image on the right is a simulation of what a person with the curve corresponding to 20/136 visual acuity shown in figure 13 on page 18 sees when looking at image on left.



Figure 19. The image on the right is a simulation of what a person with the curve corresponding to normal visual acuity shown in figure 13 on page 18 sees when looking at image on left.

## 2.7 *Digital Enhancement*

Peli and Peli first introduced the concept of using digital image processing to enhance images presented to patients suffering from visual degradation in 1984 (26). The initial model of a person's visual loss they used was the contrast sensitivity function (CSF) which was the inverse of the contrast threshold curve which represented the minimum contrast, or amplitude, necessary for a person to resolve whether sinusoidal intensity gratings at various frequencies

were horizontally or vertically oriented. They measured the CSF in various patients and used them to calculate individual visual degradation transfer functions (VDTF), which were the ratio of the CSF of the patients with cataractous vision to the CSF of persons with normal vision. Peli decided that using the VDTF as an inverse filter produced too much “salt and pepper” noise due to the amplification of the higher frequencies attenuated by a degraded visual system. He instead conjectured that adaptive image enhancement (27) (see below) may be better for enhancement. Although no testing was done in 1984 to see the effects of these enhancements on patients, the effects of inverse filter enhancement as viewed through simulated cataractous conditions were studied. In their paper on computerized image enhancement (22), Peli and others addressed: contrast manipulation, spatial filtering, and pseudocolor recoding. In her paper on attempts to improve reading rates in the visually impaired, Lawton discussed using the contrast sensitivity function as a compensation filter (15). Peli once again tackled enhancement using a pre-emphasis filter concept (21) in his 1992 paper on limitations of image enhancement.

*2.7.1 Contrast Manipulation.* Contrast manipulation involved using the dynamic range of a display device to redistribute the contrast information in such a way so that it was more useful to the observer. Two types of contrast manipulation were “histogram equalization and hyperbolization”, and “thresholding”. Histogram equalization forced the image’s gray scale values to yield a flat histogram. The image on the right in figure 20 is the histogram equalized version of the low contrast image on the left in the same figure. Peli pointed out, though, that histogram equalization could sometimes cause a loss of information since bright



Figure 20. Result of histogram equalization on a low contrast image.

regions in the original image may become very bright after equalization. Hyperbolization forced the values into a hyperbolic shaped histogram and had less of the brightening effect of histogram equalization. Thresholding, used in many applications for segmenting information in an image, yielded the outline of the person in the original image and preserved much of the information as shown in the left image in figure 21. The middle image of figure 21 is the result of passing the image through the previous simulation of what a person with 20/136 vision sees when looking at the image on the left. Adaptive thresholding (24) involved



Figure 21. Left: Result of thresholding in original image. Middle: Simulation of what a person with the curve corresponding to 20/136 visual acuity shown in figure 13 on page 18 sees when looking at image on left. Right: Simulation of what that same person sees when looking at the original, un-enhanced image.

dividing an image into non-overlapping sections. Each section was evaluated to determine its appropriate threshold and every pixel in the image was then thresholded based on threshold values interpolated between the sections. Peli stated one drawback to this method was that some patients complained that thresholding as an enhancement technique caused the resulting image to look "cartoonish."

**2.7.2 Spatial Filtering.** Image enhancement by spatial filtering would optimally amplify those spatial frequencies most attenuated by the visual system of the afflicted patient. At the time of this thesis, Peli was investigating the use of the VDTF in an inverse filter enhancement technique (21). He mentioned a number of enhancements which would boost the high frequency information in an image. High-pass image filtering techniques included: unsharp masking, extremum sharpening, and adaptive filtering. Unsharp masking subtracted a low-pass version of the image from the original. Extremum sharpening passed a spatial

mask over the original image; the points inside this mask were assigned the maximum or minimum pixel value in the window, depending on which value the current pixel was closest to. Adaptive image enhancement involved low-pass filtering the original image, subtracting this lpf image from the original image, and adding this new image (which contained high frequency information) to the original. The effects of this technique are shown in figure 22; on the left of this figure is the enhanced image, while in the middle is the enhanced image as



Figure 22. Left: Result of Adaptive filtering original image. Middle: Simulation of what a person with the curve corresponding to 20/136 visual acuity shown in figure 13 on page 18 sees when looking at image on left. Right: Simulation of what that same person sees when looking at the original, unenhanced image.

seen by the low vision observer with visual acuity of 20/136 shown in figure 13. Comparing the image in the middle to the unenhanced perceived image on the right, notice that many of the facial characteristics have been recovered and that the enhanced image may be more recognizable to the low vision patient. Adaptive filtering was the same as adaptive image enhancement.

Peli tested adaptive image enhancement and adaptive thresholding in 1991 on patients suffering from low vision (24). He used parametric estimation by sequential testing (PEST) (28, 16) to minimize the number of measurements necessary to determine each patient's CSF. These enhancement techniques were not tuned for a specific patient's CSF, but were tuned to enhance the frequencies above 4 cycles per image which were most useful for face recognition. The results of the testing indicated that 39 out of 46 patients tested had better facial recognition ability when viewing the enhanced faces than when viewing the un-enhanced faces.

**2.7.3 Pseudocolor Recoding.** Images could be enhanced using pseudocolor recoding, which would take advantage of the extra information contained in the “hues” of the image. Subjects, though, would need to be retrained to the new color representations. Also, damage of the macula lutea implies damage near the fovea, the area containing the highest concentration of the cones which detect color. Therefore, this technique would probably prove itself less than optimal for improving recognition ability in those suffering from low-vision due to macular degeneration.

**2.7.4 Compensation Filters.** In her 1988 paper (15), Lawton described her attempt at improving word recognition in three low-vision patients using compensation filters based directly on each individual patient’s CSF normalized to a normal viewer’s CSF. She used this normalized CSF (NCSF) essentially as an inverse filter, directly correlating the amount of gain at a particular frequency to the inverse of the NCSF at that spatial frequency. The compensation filter used was of the form,

$$\frac{NCSF}{NCSF^2 + \frac{1}{Gain^2}}, \quad (4)$$

where *Gain* determined how much of a tradeoff there was to be between amplification of high frequency noise and a noise-free image. In her experiment, only letters were enhanced, not faces. Testing of this technique revealed that enhancing the words with the compensation filters allowed recognition that would have required a 27-70% magnification of the un-enhanced word.

The left image in the figure 23 was obtained by using a compensation filter generated from the two curves in figure 13 on page 18, one representing normal vision and one representing the vision of the person with 20/136 visual acuity. The NCSF was the normal threshold curve point-by-point divided by the low-vision curve. The gain in equation 4 was set at 1000, which caused the compensation filter to behave as an inverse filter. To avoid divide-by-zero



Figure 23. Left: Result of applying compensation filter on original image. Middle: Simulation of what a person with the curve corresponding to 20/136 visual acuity shown in figure 13 on page 18 sees when looking at image on left. Right: Simulation of what that same person sees when looking at the original, unenhanced image.

problems, frequencies above 32 cpi were set to zero during the filter generating process. A cross section of the compensation filter used for enhancement is shown in figure 24. The

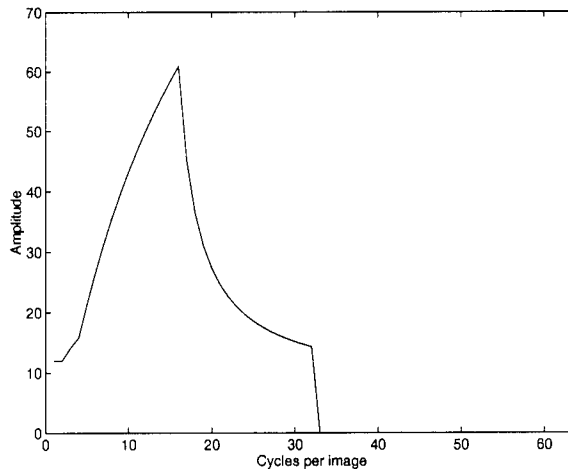


Figure 24. Cross section of compensation filter used for enhancement.

resulting enhanced image was histogram equalized so that the pixel values would lie between 0 and 500. This resulted in saturation of some of the pixels since the picture was displayed with a dynamic range between 0 and 255.

In 1994, Fine and others attempted to reproduce the results obtained by Lawton in her experiment concerning improved reading rates in the visually impaired (7). Although they could not reproduce her results precisely, they were able to find a significant increase in the

reading rates of individuals viewing enhanced text. Fine used letters similar in appearance to Lawton's. Conjecturing that Lawton's enhancement technique may have enlarged the letters, they set up a test to find out if larger letters would lead to the same increase in reading rate as Lawton's technique. It was seen that simply enlarging the letters did not lead to the same increase in reading rate, thereby arguing the possible usefulness of using the normalized contrast sensitivity function as an inverse filter.

#### *2.7.5 Modified Pre-Emphasis Model.*

Peli's most recent image enhancement endeavor involved using a band-emphasis filter to boost frequencies most useful for face recognition in a given subject (21). The image was first low-pass filtered to remove all frequencies unusable by the subject. An emphasis filter was built to boost the highest frequency seen by the subject, while leaving untouched the frequencies below that highest frequency. The amount to boost the high frequency was determined by the ratio of the subject's contrast threshold to a normal contrast threshold at that frequency. Peli left the lower frequencies untouched for aesthetic reasons since those frequencies kept the enhanced image from looking like a line-drawing. The filter used is shown in figure 25. It was also pointed out that some

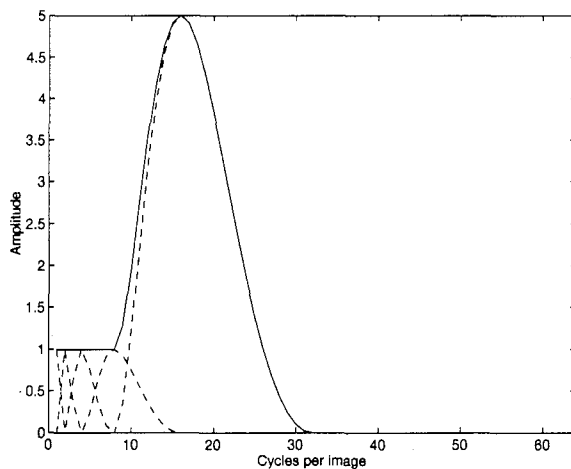


Figure 25. Pre-emphasis filter used for enhancement.

saturation of the pixel values in the resulting enhanced image allowed more information to be displayed than if straight histogram equalization to the full dynamic range of the display

was used. As an example, if the frequencies of the original image are multiplied by the pre-emphasis filter shown in figure 25 and then histogram equalized to stretch the pixel values between 0 and 800, the left image in figure 26 is the result. That image is the enhanced image



Figure 26. Left: Result of applying pre-emphasis filter on original image. Middle: Simulation of what a person with the curve corresponding to 20/136 visual acuity shown in figure 13 on page 18 sees when looking at image on left. Right: Simulation of what that same person sees when looking at the original, unenhanced image.

presented to the subject, while the image in the middle is the simulated image perceived by a person with 20/136 vision shown in the threshold curve of figure 13. Once again, notice that the middle image may be more recognizable than the un-enhanced perceived image on the right.

## 2.8 Wavelets

The previously mentioned enhancement techniques represent a large and useful arsenal in the fight to restore recognition abilities in those with low-vision. The most promising of the above rely on direct manipulation of an image's spatial frequency spectrum. Some theories involving the way mammalian brains process auditory (35) and visual (12, 13) information suggest that human perception can be modelled with wavelet analysis. The significance of discrete wavelet analysis compared to discrete Fourier analysis lies in the decomposition and reconstruction process inherent to wavelet analysis. Here, it is seen that discrete wavelet analysis can be used as a tool for image enhancement and for simulating human perception of an image using a particular contrast sensitivity function.

In his paper on contrast in complex images, Peli mentioned image analysis and synthesis schemes using his log cosine implementation to determine band-limited contrast (24). One analysis scheme that has not been used, one that may more closely represent visual processing, is wavelet analysis. Discrete wavelet coefficient sets can be thought of as images that have been filtered in the frequency domain with filters having cutoffs at powers of two and bandwidths of one octave. This section explains discrete wavelet implementation from a non-mathematically rigorous, very practical standpoint. For a more mathematically intense analysis of two dimensional wavelet theory, an excellent overview is presented in the paper by Mallat (18) and in the Masters Thesis by Laing (14) (A note concerning the Laing Thesis; in figures 36 and 38, both explaining the mechanics of wavelet reconstruction, the upsampling occurs after convolution. This is incorrect, although it is explained correctly in his text; the convolution must occur after the upsampling, thus maintaining the reconstruction as the mirror operation of the decomposition).

To decompose an image using the standard discrete wavelet transform (DWT), two one-dimensional vectors are necessary: a vector representing the scaling function and a vector representing the wavelet function. The vector representing the scaling function is usually denoted as  $h$  and has a frequency response displaying low-pass characteristics. The vector representing the wavelet function is usually denoted as  $g$  and has a frequency response displaying high-pass characteristics.  $h$  and  $g$  form an orthogonal basis set.

With simple *orthogonal* wavelets, a single vector is given for the scaling function. The wavelet coefficients vector is generated from the scaling coefficients using the relationship,

$$g(n) = -1^{1-n} \times h(1-n). \quad (5)$$

Now that these two vectors are available, the actual image decomposition is accomplished by using the mirrors of these two vectors; that is,  $\tilde{h}(x) = h(-x)$  and  $\tilde{g}(x) = g(-x)$  are the vectors that are actually used in the decomposition operation shown in figure 28.

The wavelet set used in this research was the *biorthogonal* wavelet set used by the FBI for image compression of fingerprint data (10, 37, 17). This set was chosen because the decomposition functions were symmetric about zero, which meant that manipulations of the detail coefficients would not cause distortion of the reconstructed image (as may be experienced using other compactly supported, non-symmetric wavelet sets). Using biorthogonal wavelets required a slightly different approach than that for orthogonal wavelets sets outlined in Laing's thesis. With a biorthogonal wavelet set, *two* vectors (used for decomposition) are initially given. One vector given represents the scaling function to use for decomposing an image ( $\tilde{h}$ ) and the other vector given represents the wavelet function used for decomposition ( $\tilde{g}$ ). The biorthogonal vectors shown in tables 1 and 2 were the ones used by the FBI for fingerprint encoding and were obtained from the Thesis by MacDonald (17). The waveforms corresponding to these vectors, used for decomposition, and their relationship are shown in figure 27. Notice that figure 27 seems to indicate that non-zero values for the scaling and

Table 1. Coefficients for the scaling function used in the forward wavelet decomposition ( $\tilde{h}$ )

Position	Approximate Value
$\tilde{h}_0$	+0.85269867900940
$\tilde{h}_{\pm 1}$	+0.37740285561265
$\tilde{h}_{\pm 2}$	-0.11062440441842
$\tilde{h}_{\pm 3}$	-0.023849465019380
$\tilde{h}_{\pm 4}$	+0.037828455506995

Table 2. Coefficients for the wavelet function used in the forward wavelet decomposition ( $\tilde{g}$ )

Position	Approximate Value
$\tilde{g}_{-1}$	+0.78848561640566
$\tilde{g}_{-2,0}$	-0.41809227322221
$\tilde{g}_{-3,1}$	-0.040689417609558
$\tilde{g}_{-4,2}$	+0.064538882628938

wavelet functions occur only at positive indices. This is an artifact of using Matlab for the analysis. The scaling function ( $\tilde{h}$ ) is symmetric about zero, and the wavelet function ( $\tilde{g}$ ) is symmetric about minus one. Figure 28 shows the decomposition process for an image.

Decomposing an  $N \times N$  image involved implementing the following steps:

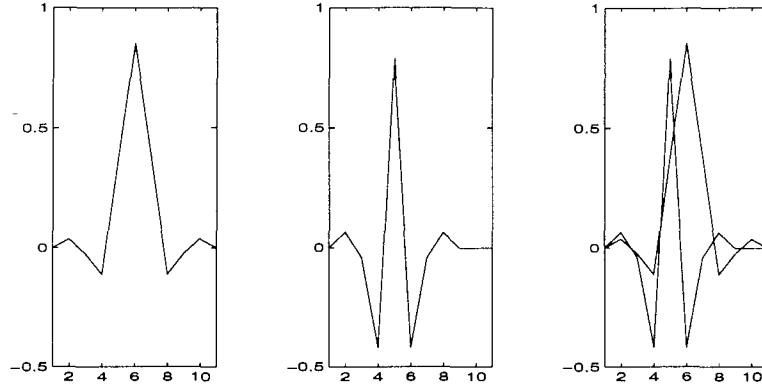


Figure 27. Decomposition scale function ( $\tilde{h}$ ) is on the left, decomposition wavelet function ( $\tilde{g}$ ) is in the middle, while their relationship is shown on the right.

1. Generate a column coefficient set by convolving the columns of the image with  $\tilde{g}$ ; generate another column coefficient set by convolving the columns of the image with  $\tilde{h}$ . The convolution of the first column in the image with the scale function is defined as

$$\text{Column}_i * \tilde{h} = \sum_{m=1}^N \text{Column}_m \tilde{h}_{i-m}, \quad (6)$$

This convolution is circular; that is to say that when the vector encounters the image's edge, it wraps around to the other side of the image.

2. Downsample the columns of each of these coefficient sets by keeping every other row. The size of each image matrix is now  $N/2 \times N$ .
3. Generate two coefficient sets by convolving the rows of each of the two downsampled column coefficient sets with  $\tilde{g}$ ; generate two more coefficient sets by convolving the rows of each of the two downsampled column coefficient sets with  $\tilde{h}$ .
4. Downsample the rows of each of these coefficient sets by keeping every other column. The sizes of each of the four new matrices is now  $N/2 \times N/2$ .

The detail coefficients obtained during a wavelet decomposition can be thought of in the frequency domain as multiplying the high frequency components of the original image by a one-octave-wide band-pass filter (5). The cutoffs of this bpf are always a power of two when

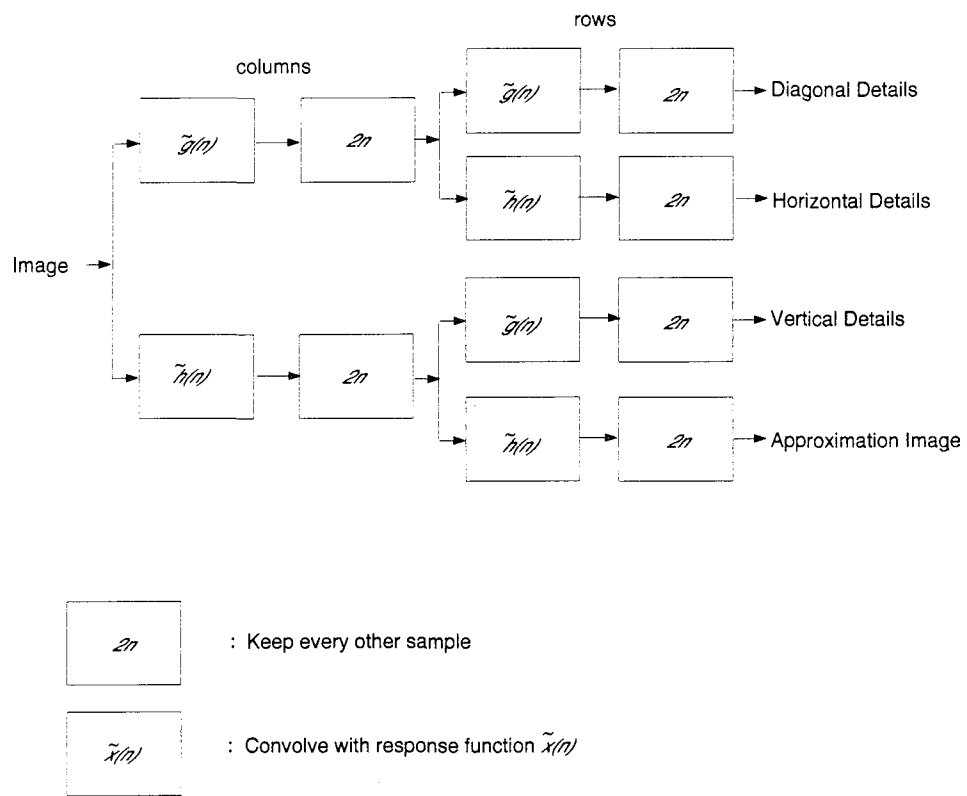


Figure 28. Decomposition flow chart to obtain first level of decomposition

the original matrix has dimensions that are powers of two. For example, the image shown in figure 15 is of size  $128 \times 128$ . The detail coefficients obtained by decomposing the image into its first level are band-pass filtered by a filter centered at 48 cycles per image with cutoff frequencies of 32 and 64 cpi (octave). See figure 29.

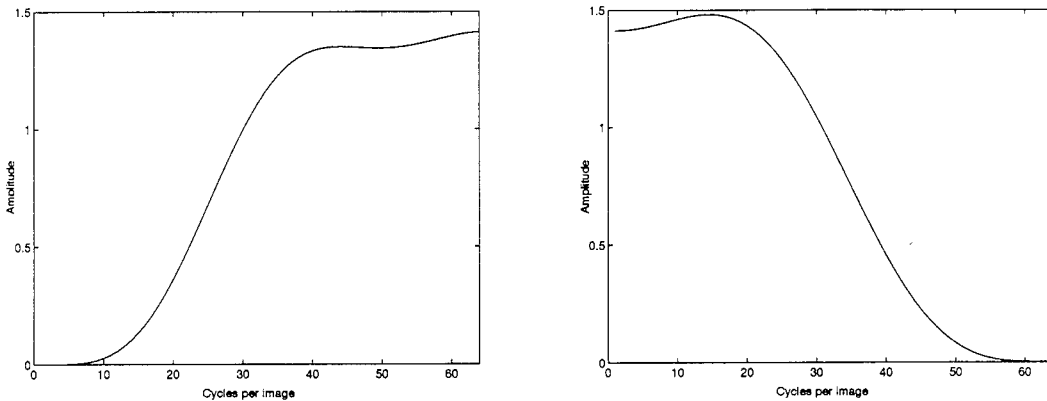


Figure 29. Left: Wavelet high-pass filter centered at 48 cpi, Right: Scale low-pass filter associated with the hpf on left

Applying the previous steps to the original image (defined as the zeroth level approximation coefficient set) yielded the first level of decomposition coefficients. To obtain additional levels of decomposition, the resulting approximation image was treated as the image and decomposed. If the image shown in figure 15 on page 20 was passed through the algorithm outlined in figure 28, each decomposition level would produce an approximation image related to the other approximation images as shown in figure 30.

The waveforms used for reconstruction ( $h$  and  $g$ ) were calculated from their decomposition counterparts ( $\tilde{g}$  and  $\tilde{h}$ ) using equation 5; that is  $\tilde{g}$  was used to generate  $h$  and  $\tilde{h}$  was used to generate  $g$ . These new waveforms were used for reconstruction and their relationship is shown in figure 31.

Reconstruction of the original image was the mirror operation of decomposition. Figure 32 shows the process of reconstructing an image after wavelet decomposition. The exact steps to follow for reconstruction of an image decomposed down to an  $N \times N$  matrix are:

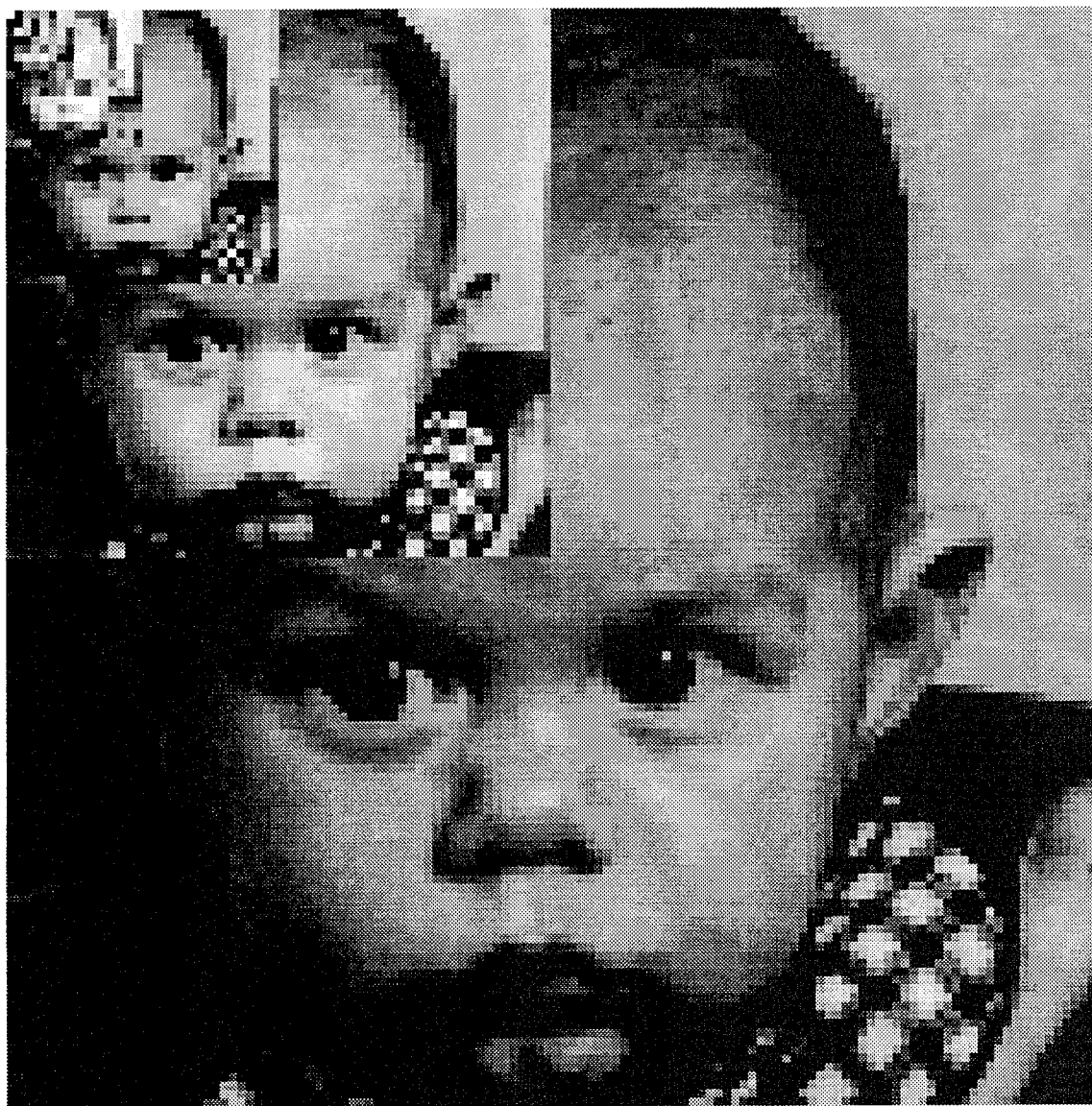


Figure 30. The relationships between the approximation images at each of the seven levels of decomposition of the original image (largest image above). Each of the above images would serve as the input image in the algorithm of figure 28. These images were all histogram equalized for presentation purposes.

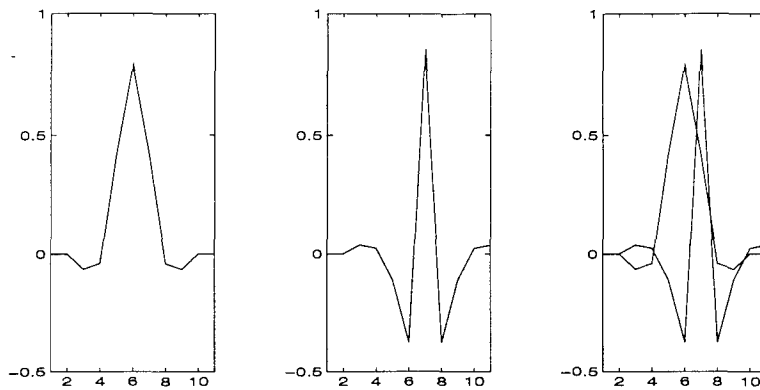


Figure 31. Reconstruction scale function ( $\tilde{h}$ ) is on the left, reconstruction wavelet function ( $\tilde{g}$ ) is in the middle, while their relationship is shown on the right.

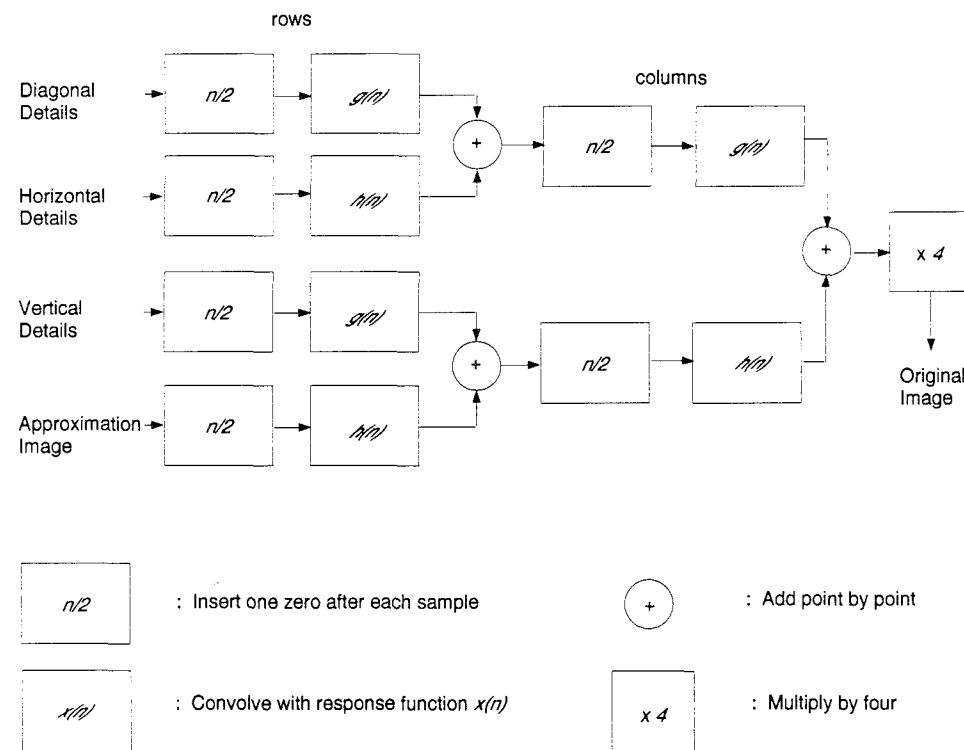


Figure 32. Reconstruction of an image after a single level of decomposition

1. Upsample the rows of each of these coefficient sets by inserting a zeros column between every column. The sizes of each new matrix is now  $N \times 2N$ .
2. Convolve the rows of the Approximation and Horizontal coefficient set with  $h$  and the rows of the Vertical and Diagonal coefficient with  $g$ .
3. Add convolved Approximation image and Vertical details image point-by-point. Add convolved Horizontal details image and Diagonal details image point-by-point.
4. Upsample the columns of each of these coefficient sets by inserting a zeros row between every row.
5. Generate a column coefficient set by convolving the columns of the Approximation/Vertical information image with  $g$ ; generate another column coefficient set by convolving the columns of the Horizontal/Diagonal information image with  $h$ .
6. Add these two remaining matrices point-by-point. The size of the matrix is now  $2N \times 2N$ .

The resulting image after the above operation became the approximation image for the next higher level of decomposition, and was combined in an identical way with the detail coefficients at the next higher level. For example, if the original image was decomposed down to the third level, reconstruction would first involve performing figure 32 on the set of four matrices representing the third level of decomposition. The output image of that operation would then become the approximation image for the three matrices representing the second level detail coefficients (horizontal, vertical, and diagonal) of decomposition and figure 32 would be performed on those four sets. The output of that operation would become the first level approximation and combined with the first level details to produce the original image. Appendix C shows the specific Matlab code used to implement this biorthogonal wavelet set for two dimensional images.

## 2.9 Headset

The headset intended to be the output for image enhancement for this thesis was the PT-01; a display system which could be raised just above the line of sight and not obstruct peripheral vision, or lowered to cover the eyes completely. It contained two active matrix 420x230 pixel screens. Each pixel was an RGB unit containing triads of three cells and occupying less than 3.2 arc minutes in size. Using the square area of 230x230 pixels located in the center of the displays, the total area would correspond to 12.3x12.3 degrees of arc. Therefore, one cycle per degree equaled 12.3 cycles per image. See figure 33.

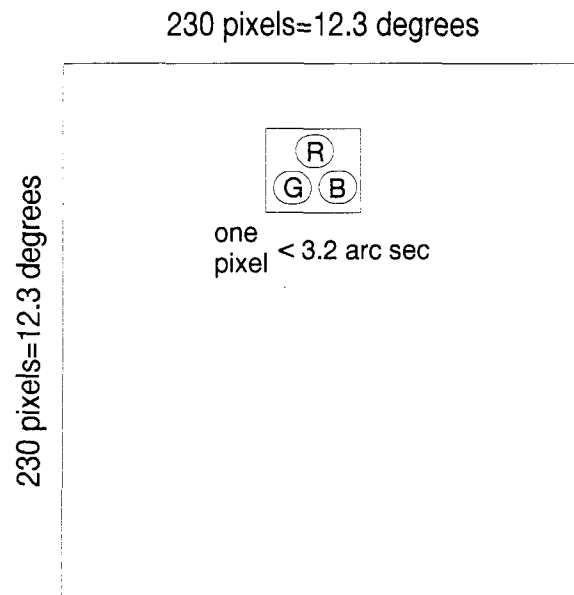


Figure 33. Active matrix LCD used in headset.

## 2.10 Summary

Millions of people suffer from low vision due to macular degeneration. Knowledge of a low vision observers visual characteristics could perhaps be used to enhance that person's view of the world so that face recognition could be improved. Peli had good success with improving the recognition abilities of low vision patients using adaptive thresholding and adaptive filtering; he also provided a simulation which could give those with normal vision

an insight into what a person with a less than optimum contrast threshold response sees when looking at a given image. Lawton and Fine demonstrated that compensation filters used to enhance words improved the word recognition rate in low vision observers. The discrete wavelet transform (DWT) was seen to break an image into different resolution information while preserving location information.

The next chapter outlines some new wavelet techniques concerning optimal image enhancement for the visually impaired and a new wavelet human perception simulation.

### *III. Methodology*

The research area outlined here was new to AFIT. This chapter presents wavelet analysis methods that will be compared to Peli's work concerning simulations of visual perception given a particular contrast threshold curve. It also presents image enhancement methods that use a given set of individual contrast perception curves to influence frequency analysis and wavelet analysis. A new method using suprathreshold characteristics of a patient to enhance an image is also presented as is an idea concerning localizing the enhancement.

#### *3.1 Wavelets*

In a practical sense, the two-dimensional Discrete Wavelet Transform (DWT) breaks an image into a set of images corresponding to different resolution information contained in the original image. For example, if the original image was contained in a 128x128 array, a wavelet decomposition would generate four new images in 64x64 arrays, four in 32x32 arrays, four in 16x16, four in 8x8, four in 4x4, four in 2x2, and four in 1x1 arrays. One array in each set of four would correspond to low frequency information, and the other three arrays would correspond to high frequency information.

The method by which an image was decomposed by the DWT lent itself readily to the analysis performed on contrast in complex images by Peli (19). When he analyzed his image of Cary Grant he used the log cosine filters shown in figure 16 on page 21. One of the most useful aspects of the DWT is its ability to locate frequency information at specific locations in the original image. Peli's band-pass filters had center frequencies at powers of two and were one octave wide (i.e. the filter to capture the information around 16 cycles per image was centered at 16 cpi with cutoffs at 12 and 24 cpi); analogous wavelet filters were one octave wide with cutoff frequencies at powers of two (for example, the filter to capture the information around 12 cpi was centered at 12 cpi with cutoffs at 8 and 16 cpi). Figures 34 and 35 display the filters of the parenthetic examples above. It is important to remember that

the reason for the upper cutoff of the high-pass frequency response of the wavelet is that the highest frequency is limited by the size of the image matrix.

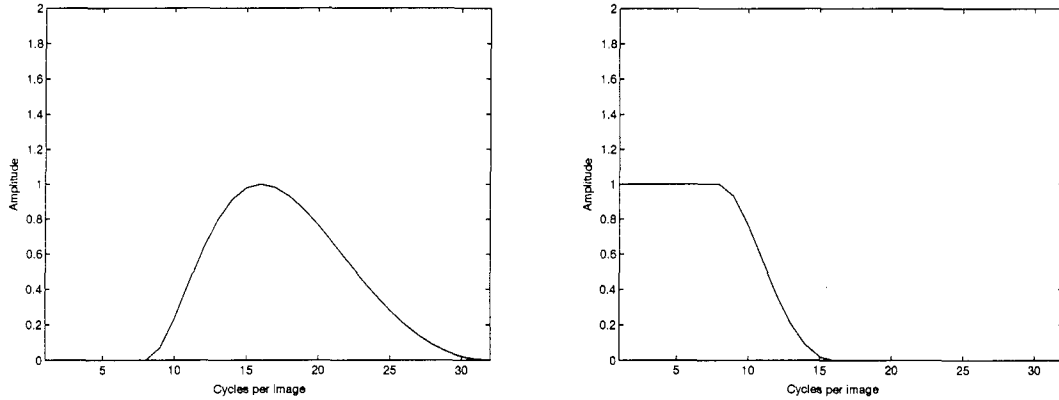


Figure 34. Left: High-pass log-cosine filter centered at 16 cpi, Right: Low-pass log-cosine filter associated with the hpf on left.

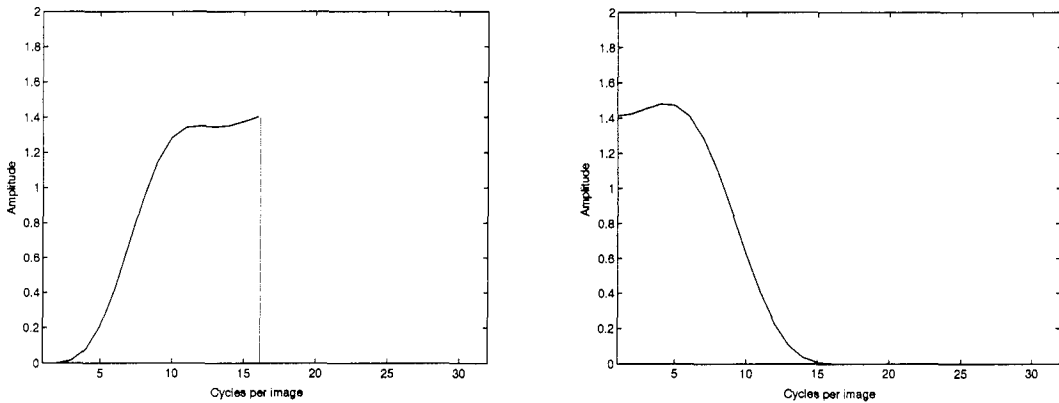


Figure 35. Left: High-pass wavelet filter centered at 12 cpi, Right: Low-pass wavelet filter associated with the hpf on left.

Since the discrete wavelet transform used circular convolution on the rows and columns during decomposition and reconstruction, edge effects became apparent whenever the detail coefficients were manipulated. The solution used in this thesis was to implement an algorithm by Cohen and do the DWT on a “mirror quad image,” such as the one shown on the right in figure 36, instead of the original image shown on the left (5). This operation did not effect

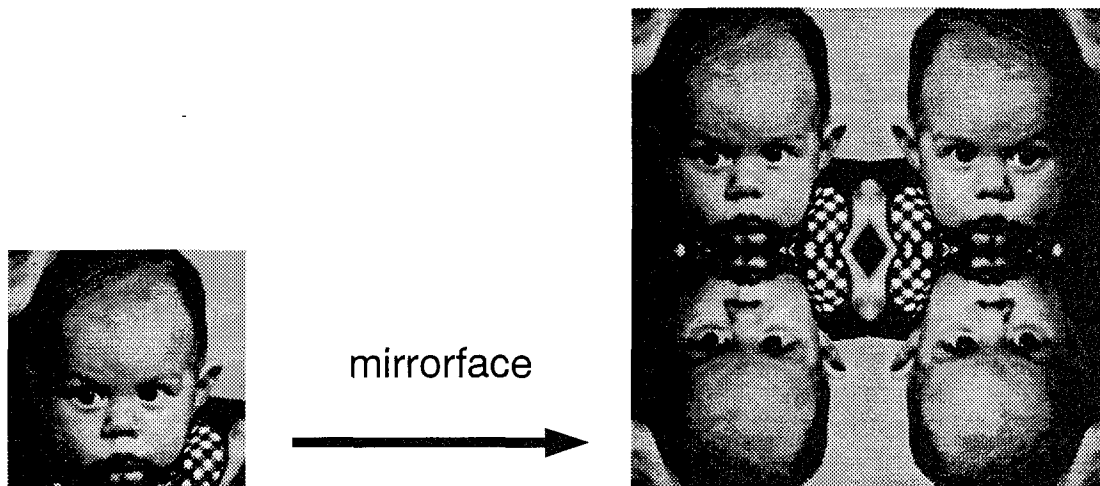


Figure 36. Mirror quad image (size 256 x 256) transformation of original image. The image on the right was the actual input into the algorithm outlined in figure 28 on page 34.

what resolution information was contained in each of the coefficient sets. For example, for the original 128 x 128 image, the first approximation yielded a low-pass filtered version of the original with cutoff frequency of 32 cycles per image. Using the mirror quad operation, the first approximation was a low-pass filtered version of the mirror quad image with cutoff frequency of 64 cycles per mirror quad image, but this same cutoff was still 32 cycles per *original* image. The decomposition approximation and detail coefficients remained in the mirror quad format during any analysis of the information.

An important consideration after reconstruction was that the reconstructed, manipulated final image was a reconstructed mirror quad image; this image, though, was not truly a mirror quad image due to the various manipulations encountered between decomposition and reconstruction. To maintain manipulated information from each quadrant of the final image, the displayed image was an average of the quadrants of the reconstructed mirror quad image.

### 3.2 Wavelet Simulations

This section outlines how the bi-orthogonal wavelet set was used to parallel the work done by Peli concerning simulation of image perception by a subject with a given contrast sensitivity curve (19).

The first step in the process was to generate a set of images filtered from the original using octave-wide band-pass filters and corresponding low-pass filters which captured the information under the band-pass filters. Wavelet decomposition levels provided the ideal relationship in that there were coefficient sets containing detail information about the image at different resolutions which could be compared to the approximation coefficient set at that level. For example, the third level details (shown in figure 37) were each point-by-point

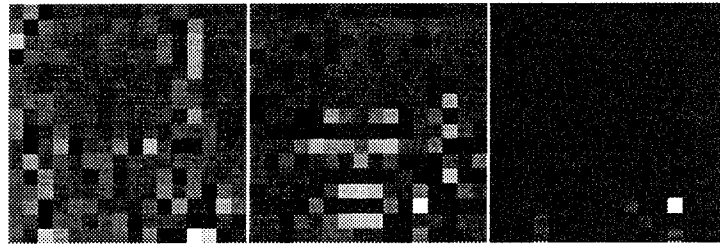


Figure 37. The first image above contains the third level vertical detail coefficients, the second is the horizontal detail coefficient set, and the last image is the diagonal detail coefficient set.

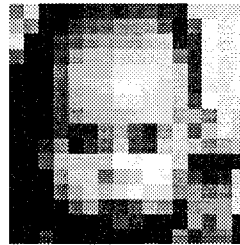


Figure 38. The image above is the third level decomposition approximation coefficient set.

divided by the approximation coefficients in figure 38, the end result being three contrast images representing vertical, horizontal, and diagonal contrasts at those pixel positions at that level of decomposition. This first step required some subtle manipulations while decomposing

the original image. The third level decomposition sets would appear as in figures 37 and 38 (discounting the mirror quad operation); however, it was inappropriate to use these for the simulation due to the shifting and downsampling imposed by the wavelet decomposition. Referring back to figure 27, notice that the wavelet function ( $\tilde{g}$ ) is not symmetric about the same point as the scaling function ( $\tilde{h}$ ). Whenever an image is being decomposed, the information will not be shifted by the convolution with the scale function since it is symmetric about zero; however, the convolution with the wavelet function produces a shift of the information since the wavelet function is symmetric about the first index to the left of zero. In order to parallel Dr. Peli's log-cosine filter analysis, each of the detail coefficient sets at each level were to be divided by the approximation image at that level; this division would yield a "resolution limited contrast image." Since the convolution with the wavelet function would shift the resulting detail coefficients with respect to the rows and columns convolved with the scale function, this shifting aspect had to be eliminated during the resolution limited contrast image generation stage. In order to eliminate this shifting during convolution, the wavelet was forced to center at zero. Figure 39 shows the new, modified scale and wavelet vectors used in the wavelet simulation decomposition and figure 40 shows how the un-shifted detail coefficient sets were generated. Compare figure 39 to figure 27 on page 33 and notice that the functions

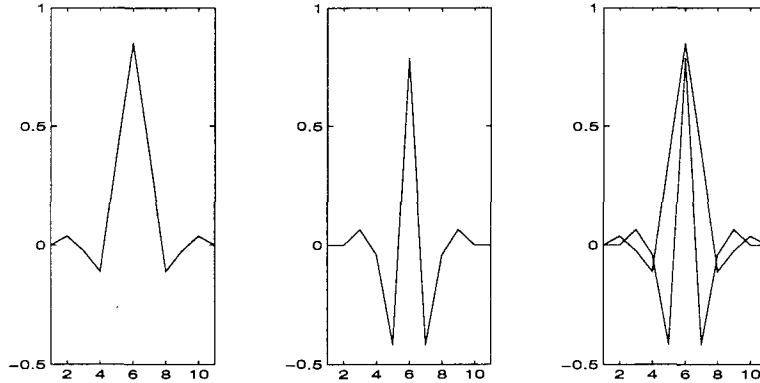


Figure 39. Scale function (at left) and un-shifted wavelet function (middle) used in wavelet Simulation. Their relationship is shown in the plot on the right.)

are the same, only the indexing is different. This new wavelet decomposition set was then

convolved with the rows and columns; this allowed the resolution limited contrast images to be calculated with the positions of all the decomposition images correctly aligned relative to one another.

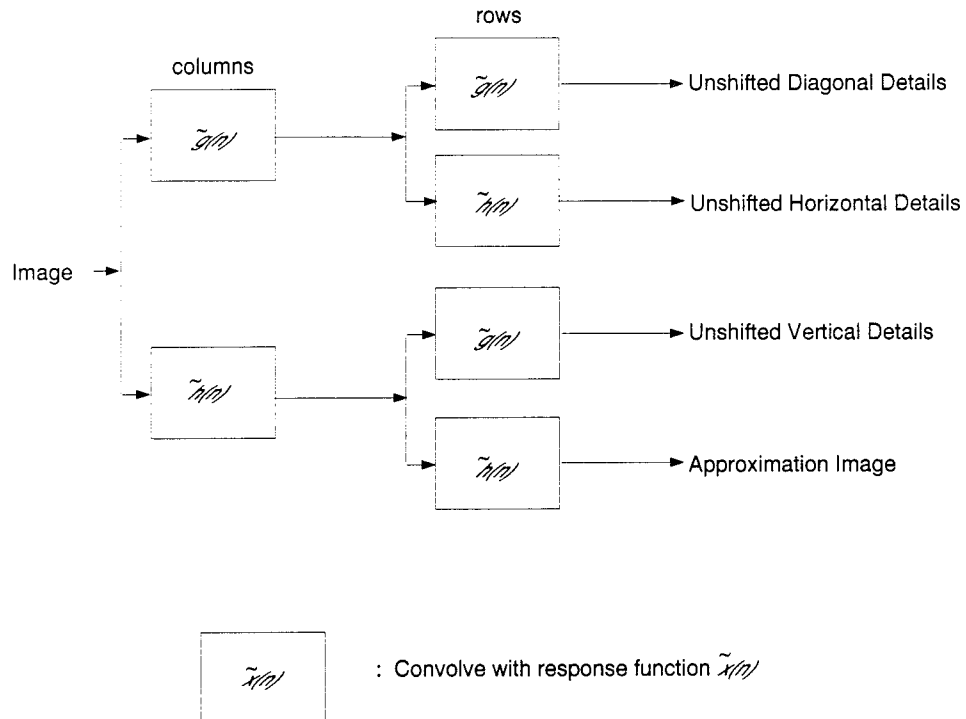


Figure 40. Generation of un-shifted detail coefficients.

The result of using the algorithm of figure 40 was that the first level of decomposition yielded four matrices that were the same size as the original image matrix, and those four matrices were used to compute the resolution limited contrast images.

These resolution limited contrast images were compared point-by-point to the proper threshold value (interpolated from the contrast threshold curve in figure 13 on page 18 used for the other simulations). If the value was at or above threshold, the detail coefficient at that location was left alone. Otherwise, if the value was below threshold, the detail coefficient at that location was set to zero. For example, a set of resolution limited contrast images corresponding to 12 cycles per image was generated, using the coefficient sets in the third level decomposition (shown in figure 37 and 38) by dividing each of the three third level detail

coefficient sets point-by-point by the third level approximation image. These three contrast images were point-by-point compared to the value interpolated at 12 cpi from the plot for the person with 20/136 vision shown in figure 13 on page 18 (that threshold value was .4096). If the value at that coordinate position in the detail contrast image was below threshold, the pixel value in the corresponding detail coefficient matrix was set to zero. This represented a loss of detail at that coordinate position. If the value at that coordinate position in the detail contrast image was above threshold, the value in the corresponding detail coefficient set was left untouched.

It was at this point in the process where downsampling occurred. The critical shift that was eliminated previously now had to be reinserted because it was vital to the reconstruction process. This algorithm did the shifting during the downsampling process instead of during the convolution with the wavelet function; the downsampling of any column or row convolved with the scaling function took the even indices starting with index two, while the downsampling of any column or row convolved with the wavelet function took the odd indices starting with index three (the last index being index one due to circular convolution). Figure 41 shows how the downsampling was used to implement the shifting. This preserved the information storage aspect of the wavelet decomposition and allowed reconstruction to occur in the normal fashion as shown in figure 32 on page 37.

This process was repeated at all resolution levels down to the smallest resolution level with detail coefficients which had maximum resolution of 4 cycles per image (which resulted in a 4 x 4 image after downsampling), and then reconstructed in the standard fashion of the biorthogonal wavelet, as shown in figure 32 on page 37. Appendix D contains the Matlab code used for these simulations.

### 3.3 Wavelet Enhancement

In order to maintain the flow of the work already accomplished by Dr. Peli, the first wavelet enhancement technique explored here paralleled his modified pre-emphasis filter enhancement technique. The pre-emphasis model boosted the highest frequencies the subject

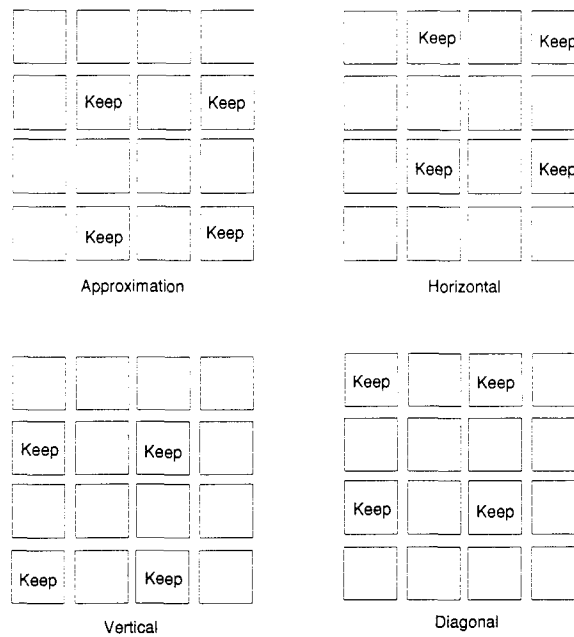


Figure 41. Method by which the downsampling was used to achieve the shifting normally accomplished by the wavelet.

could see by the inverse of the normalized threshold measured at that frequency for that person. For the wavelet case, the boosting was done to the highest detail coefficients the person would be able to discern. In Dr. Peli's paper in which the pre-emphasis model is presented (24), the example centered the boosting frequency at 16 cycles per image. The wavelet model presented here boosted the frequencies centered at 12 cycles per image; this new center frequency was determined by the nature of the discrete wavelet decomposition. Figures 37 and 38 show the third level detail coefficients and the third level approximation coefficients. With the detail coefficients generated down to the desired level to be boosted (here that was level three), each detail coefficient set was multiplied by whatever the enhancement algorithm called for at each specific resolution based on an individual's perception characteristics (here the third level detail coefficients were multiplied by a factor of five). Each of the three detail levels (horizontal, vertical, and diagonal) were multiplied by the same number, since the combination of the three corresponded to a band-pass filtered image.

### *3.4 Using Individual Suprathreshold Contrast Characteristics of a Patient for Enhancement*

Peli's early work in digital image enhancement relied heavily on boosting frequencies most useful for face recognition without regard for a particular person's visual characteristics (26, 22, 24). His and other's later experimentation on tailoring enhancement to the individual was based on measuring contrast threshold characteristics of a patient and using that information for enhancement (15, 19, 21, 24, 7). Rubin argued (based on testing of both young and old observers) that the contrast sensitivity of a low vision observer may not in fact predict recognition ability (31); here it is proposed that suprathreshold characteristics of a subject would be more useful for image enhancement. The contrast in facial images is usually above the threshold of normal observers. Using contrast sensitivity, which is based on contrast threshold, for enhancement may not optimize the information in the image that the subject *can* see. Suprathreshold contrast perception curves, close to threshold, tend to be shaped the same as the threshold curve; but as the contrast increases, the relationship between the perceived suprathreshold contrasts changes. If the suprathreshold contrast perception of the subject was used to enhance the image instead of the threshold contrast perception, this would more efficiently enhance those frequencies dominant in the image. The remainder of this section describes a new method of image enhancement tailored to an individual subject using measured normalized suprathreshold curves such as those shown in figure 14 on page 19 (2).

First, the contrast information in the image had to be determined. Since Cannon's suprathreshold matching experiments (see figure 14 on page 19) indicated that 4 cycles per degree was the most sensitive frequency of those normal observers measured during that particular study, that frequency was the "reference frequency." Different measurement techniques may yield different suprathreshold contrast curves, thereby determining the actual reference frequency. The technique used to determine the contrast at that frequency took advantage of the band-limited contrast concept outlined in his paper on contrast in complex images (19). The image was band-pass filtered with Peli's log-cosine filter corresponding to 4 cpd to create the bpf image; low-pass filtered with the low-pass filter to complement that band-pass filter (analogous to the filters shown in figure 16 on page 21), and the former image

point-by-point divided by the latter. This operation created a reference contrast image for the frequency most detectable to the normal observer. The global reference contrast of the image was then determined to be the root mean square of the pixel values in the image. This global reference contrast of the 4 cpd information in the image determined which of the suprathreshold curves to use. For example, if figure 14 on page 19 was the set of curves generated by testing a low-vision subject (even though these particular curves were generated using the average of a number of normal observers), and the rms value of the reference contrast image fell closest to .01 (as opposed to .003 or .03), the curve chosen for enhancement purposes would be the first curve up from the threshold curve (where the contrast of 4 cpd was .01).

Now that the proper curve was chosen, the frequency manipulation to be performed was determined by the suprathreshold curve generated by normalizing the curve for the subject to a curve generated by a number of normal observers. This new curve was the "Normalized Contrast Suprathreshold Curve" (NCSC). Its inverse was used as an inverse filter, much in the same manner as what Lawton did in her experiments concerning improving reading rates in low-vision observers (15).

### *3.5 Localization*

Unless an observer is trying to recognize the face of a person very distant from him, the fovea of the observer will not usually encompass the entire visage of the subject of interest. The fovea covers approximately one to two degrees of arc in the visual field of view (1), and for this reason people "saccade" and scan the face of interest to get the "whole picture." This implies that, at any given time during this process, the observer is using his fovea on only a small part of the facial image; the rest of the face is still in view, but being perceived by the less visually acute retinal periphery. These facts lead to the problem of how best to locally enhance a face for individualized perception.

Global manipulation of an image wastes many precious resources: the finite dynamic range of the screen limits the possible gain of high frequencies (21); enhancement algorithms work more slowly when processing the whole scene; and the person is already placing an

object of interest in their area of highest visual acuity (24). Since only a certain amount of information is being processed at a given time as an observer peers at a facial image, one method of optimization could be to break the image into “chunks” and enhance each chunk separately and simultaneously. The weakness with this method is that the observer may not want to look only at predetermined discrete chunks of an image, but may want to choose which chunks to focus upon, saccading the image and gathering information at each stopping point. This fact implies that the optimum solution would be to enhance the image only in the area of interest to the observer.

Retina motion trackers have been developed (11, 38) which can tell precisely where each eye is looking at any given instant. Since persons with macular defects tend to place an object of interest just outside the dead area of the fovea (24), if that low vision subject were instructed to look at a point of interest corresponding to one or two degrees of arc so as to see that point in the most optimal fashion, the motion tracker could be aligned to this new “pseudo-retina.” The enhancement of a given image would then be tied directly to what the subject wanted enhanced (i.e. where the subject was looking).

### 3.6 *Metric of Enhancement Effect*

The intrinsic complexity and adaptability of the human visual system has caused more than a little consternation in the image processing community. *Image quality* is a subjective term that refuses to be tied down to a single set of numbers or equations which may allow a solid metric by which image manipulation results can be evaluated. Images of the natural world contain many frequencies and intensities for the human eye to process; add to this the restricted field of view imposed by a headset and the limited dynamic range of the output screens of the image enhancement system being viewed by the subject, and the problem becomes even more difficult.

Here, one metric of enhancement effect is proposed. Although image enhancement usefulness for any given person can only be determined experimentally, the enhancement effect metric proposed here was based on the known edge detection properties incorporated in

the average human visual system. First, the assumption was made that a simulation of human visual perception based on an individual's contrast sensitivity is representative of what that individual perceives when looking at an image. Both the Peli and wavelet simulations were used. Second, each enhancement to be evaluated was run through that simulation. Third, an edge detection algorithm was applied to the original image and the output images of the simulation. Finally, the edge detected enhanced images were compared to the edge detected original image by cross correlating the two edge-detected images; the desired result being an image perceived by the individual that is perceived to be as close as possible to the original. The edge detection convolution mask used was the Laplacian mask (9). This mask, shown in figure 42, was two-dimensionally convolved with the image of interest. This resulting image

$$\begin{matrix} & \begin{matrix} 0 & -1 & 0 \end{matrix} \\ \begin{matrix} -1 & 4 & -1 \end{matrix} & \\ & \begin{matrix} 0 & -1 & 0 \end{matrix} \end{matrix}$$

Figure 42. Laplacian convolution mask used for edge detection.

was a measure of the effective edges in the image.

As an example, using this metric to measure the effective edge enhancement of the pre-emphasis filter enhancement outlined in section 2.7.5, the first step involved detecting the edges in the original image shown on the left in figure 43. The resulting edge-detected image is shown on the right. The image on the left in figure 44 is the pre-emphasis filter enhanced image after being run through the Peli simulation, while the image on the right is the edge-detected version of the image on the left. The similarity measure was computed by performing point-by-point multiplication of the edge-detected original (on the right of figure 43) and the edge-detected enhanced-perceived image (on the right of figure 44, then



Figure 43. Left: original image. Right: edge-detected original image.



Figure 44. Left: edge-detected pre-emphasis filtered after-simulation image. Right: edge-detection resultant of image on left.

summing the resulting matrix values to yield a scalar. This scalar was divided by the scalar obtained from comparing the original to itself (autocorrelation). This operation was intended to normalize the data between zero and one. If zero, the resulting edge analysis yielded no similarity to the original image's edge analysis; if one, the edges were identical to the original. Our example above yielded a correlation value of 0.1885.

### 3.7 Summary

A biorthogonal wavelet set was used to simulate what a person with a given contrast sensitivity function sees when looking at an image. This same wavelet set was used to enhance an image in a manner analogous to Peli's modified pre-emphasis filter enhancement. A new method for image enhancement based on a subject's measured suprathreshold characteristics was outlined. Finally, the concept was proposed that the image should be enhanced only in the area of interest to the observer. The results of the wavelet simulation and enhancement are presented and analyzed in the next chapter.

## IV. Results

This chapter outlines the results of trying the various methods discussed in the previous chapter.

### 4.1 *Simulation of Macular Degeneration Using Wavelets*

When using the wavelet scheme to simulate the vision of the person with the threshold curve corresponding to acuity of 20/136, the image on the left in figure 45 was operated on and the resulting image was as shown in the middle. The image in the middle is analogous



Figure 45. Left: Original image. Middle: Wavelet simulation of what person with threshold curve corresponding to 20/136 visual acuity shown on page 18 sees when looking at image on left. Right: Peli simulation of what that same person sees.

to the image created by the Peli simulation shown on the right. Notice that the wavelet simulation indicates that less information is lost than is indicated by the Peli simulation. This is due to the fact that the reconstruction process performed by the wavelet analysis is different than the reconstruction process performed by Peli's analysis. In Peli's simulation, each image corresponding to a band-pass filtered original image was manipulated; these resulting images were then simply added together to form the image on the right. In the wavelet simulation, each image corresponding to a detail coefficient set (horizontal, vertical, or diagonal) was manipulated; these resulting coefficient sets were then recombined at each level in the standard discrete wavelet reconstruction fashion; that is to say, many convolutions were performed during the reconstruction phase that affected the final output image.

When the curve representing normal vision in figure 13 was used with the previous wavelet simulation on the presented image on the left in figure 46, the image shown in the middle is the result. Notice that even less distortion is evident than the same Peli simulation



Figure 46. Left: Original image. Middle: Wavelet simulation of what person with threshold curve representing normal vision shown on page 18 sees when looking at image on left. Right: Peli simulation of what that same person sees.

shown on the right.

Whenever the image enhanced using adaptive filtering shown on the left in figure 47 is passed through the wavelet simulation discussed above, the result is as shown in the middle image. The wavelet simulation indicates that the adaptive filtering enhancement boosts the



Figure 47. Left: Image enhanced using adaptive filtering. Middle: Wavelet simulation of what person with threshold curve corresponding to 20/136 visual acuity shown on page 18 sees when looking at image on left. Right: Peli simulation of what that same person sees.

information available to the low-vision observer. The image in the middle is analogous to the image presented on the right. The wavelet simulation seems to once again indicate that less information is lost than the Peli simulation would indicate; this being due to the reconstruction process in the wavelet analysis.

The result of running the image enhanced using Lawton's compensation filter from section 2.7.4 (shown at left in figure 48) through the wavelet simulation is shown in the middle image. Notice once again that the middle image clearly contains more information than the



Figure 48. Left: Image enhanced using compensation filtering. Middle: Wavelet simulation of what person with threshold curve corresponding to 20/136 visual acuity shown on page 18 sees when looking at image on left. Right: Peli simulation of what that same person sees.

Peli simulation image on the right indicates.

When the image enhanced using the modified pre-emphasis filter (shown on the left in figure 49) was passed through the wavelet simulation of what a person with 20/136 vision might see when looking at that image, the result was as shown in the middle image. This



Figure 49. Left: Image enhanced using modified pre-emphasis filtering, Middle: Wavelet simulation of what person with threshold curve corresponding to 20/136 visual acuity shown on page 18 sees when looking at image on left. Right: Peli simulation of what that same person sees.

image is analogous to the image shown on the right. Here, the simulated image in the middle is virtually identical to the enhanced image on the left due to the reconstruction process.

#### 4.2 Wavelet Enhancement

When the third level of details were multiplied by a factor of five, and the image reconstructed, the resulting image was as (shown on the left in figure 50), with the image in the middle in that same figure representing what a person with 20/136 visual acuity sees when viewing the image on the left according to the wavelet simulation. The image on the left is



Figure 50. Left: Original image enhanced by multiplying the third level detail coefficients by five. Middle: Wavelet simulation of what person with threshold curve corresponding to 20/136 visual acuity shown on page 18 sees when looking at image on left. Right: Peli simulation of what that same person sees.

analogous to the modified pre-emphasis filter shown in figure 26 on page 30. Comparing the images on the right of these two figures, the pre-emphasis filter seems to preserve some of the fine details associated with the original image very well, while the wavelet enhanced version preserves different information about the details.

Diverging slightly from the specific incarnation of Peli's modified pre-emphasis filter outlined in his paper on image enhancement for the visually impaired (24) by multiplying the third level coefficients by two instead of five results in the image on the left in figure 51. This enhancement proved more subtle as can be seen in the image in the middle. The sharp edges present in figure 50 have been reduced at the possible expense of detail.

#### 4.3 Metric of Enhancement Effect

The use of edge detection analysis on enhancement effectiveness using the Peli simulations resulted in values as shown in table 3, while the use of edge detection analysis on enhancement effectiveness using the wavelet simulations resulted in values as shown in ta-



Figure 51. Left: Original image enhanced by multiplying the third level detail coefficients by two. Middle: Wavelet simulation of what person with threshold curve corresponding to 20/136 visual acuity shown on page 18 sees when looking at image on left. Right: Peli simulation of what that same person sees.

ble 4. Both analyses clearly indicate that any of the outlined manipulations of the image boost the edge energy being perceived by the subject beyond what was obtained with no enhancement. The values calculated that were above one occurred with thresholding and adaptive filtering; this may indicate too much edge enhancement since subjects have complained about the thresholding technique making the image look too cartoonish. Note also that the wavelet enhancement results were roughly the same as the modified pre-emphasis filter enhancement results. This modified pre-emphasis filter is currently what is being used in the LVES at Johns-Hopkins.

Enhancement	Similarity
Original image	1
No enhancement	0.0092
Thresholding	0.1019
Adaptive filter	0.2003
Compensation filter (no histogram equalization)	0.0411
Compensation filter (histogram equalized)	0.1953
Pre-emphasis filter	0.1885
Wavelet enhance(gain=2)	0.0660
Wavelet enhance(gain=3)	0.0949
Wavelet enhance(gain=4)	0.0972
Wavelet enhance(gain=5)	0.1106

Table 3. Applying edge detection metric to perceived (Peli simulation) enhanced images.

Enhancement	Similarity
Original image	1
No enhancement	0.3154
Thresholding	1.4091
Adaptive filter	1.3047
Compensation filter (no histogram equalization)	0.4633
Compensation filter (histogram equalized)	0.3378
Pre-emphasis filter	0.3464
Wavelet enhance(gain=2)	0.4183
Wavelet enhance(gain=3)	0.4464
Wavelet enhance(gain=4)	0.4340
Wavelet enhance(gain=5)	0.4237

Table 4. Applying edge detection metric to perceived (wavelet simulation) enhanced images.

#### 4.4 Summary

The result of using a biorthogonal wavelet set to simulate the perception of a person with a given set of visual perception characteristic curves indicates that the details of an image may not be as suppressed as the simulation proposed by Peli indicates. The new enhancement algorithms using wavelets are seen to be comparable to the enhancements previously explored by Peli and others. The enhancements occur primarily along the horizontal and vertical directions, which is reasonable due to the nature of the wavelet decomposition and reconstruction. Figure 52 displays many of the enhancement techniques and the effects of running the images through the simulations. The next chapter discusses the implications of the wavelet simulations and enhancements.



Figure 52. Summary of various enhancements. The left column contains enhancements, the middle column contains the image at the left run through the Peli simulation, the right column contains the image at the far left run through the wavelet simulation

## *V. Conclusions*

### *5.1 Analysis of Algorithms Reproduced*

The previous work in the area of image interpretation and enhancement for the visually impaired concentrated primarily on the manipulation of the Fourier spectrum. One desire of past research has been to use the visual characteristics of the observer as a guide for enhancement, since those visual characteristics should be able to be compared to a normal observer's visual characteristics and the image enhanced somehow based on this knowledge. It has been conjectured that the visual system of a subject could be understood, at least in part, by non-invasively measuring the contrast threshold and suprathreshold characteristics of that subject. This research reproduced Peli's perception simulation model using the contrast threshold response of an observer to simulate the appearance of an image to that low-vision observer. This simulation was based on filtering characteristics of the human visual system and its inability to perceive those frequency components below threshold contrast. Various enhancement schemes from the literature were reproduced, most of which manipulated the Fourier spectrum of the image to make it more recognizable to the low-vision viewer. The compensation filter used by Lawton to enhance letters (15) was used to enhance faces. This research demonstrated it was a feasible tool for image enhancement. Peli's modified pre-emphasis filter enhancement, which is being used in the LVES, was reproduced and seen to also enhance the details significantly.

A practical application of the discrete wavelet transform was implemented and discussed, as was its relationship to Fourier analysis. Wavelet analysis was seen to break an image into different global resolution information sets which could be manipulated and reconstructed.

### *5.2 Analysis of Original Algorithms*

Here was proposed a new simulation of human perception based on wavelet analysis. This simulation using wavelets of what a person with a given threshold curve sees when

looking at an image yielded different results than the analogous simulation using the log cosine filters proposed by Peli. Most noticeable was the fact that more details were present in the resulting wavelet simulation images than in the Peli simulation images. Using wavelet analysis to simulate human visual perception provided a different choice for a basis set, one that is supported by recent work concerning mammalian cortical processing (12, 13, 35). The overriding concern with all of these simulations is that human perception is still poorly understood. If wavelet analysis truly does model human visual perception, then the next logical step is to determine which set of coefficients the brain uses to process that information. The wavelet simulation implies that the various enhancement algorithms presented here are, in fact, perceived by the subject. One test to measure the value of the wavelet simulation would be to have a person with normal vision in one eye and low vision in the other view an image one eye at a time and give an opinion.

Wavelets were used to provide a new image enhancement procedure by manipulating the decomposition detail coefficients. The new metric to analyze the enhancements based on edge similarity measures showed that, at least in the regard of edge enhancement, the perceived wavelet enhancements were matching the original image at about the same level as the perceived modified pre-emphasis filter enhancements proposed by Peli. The true usefulness of the wavelet coefficients as enhancement tools can only be determined by the testing process. The only sure statement that can be made about image enhancement for the visually impaired, without first having a better understanding of the human visual system, is that individual subject preferences will be the deciding factor when choosing the optimal enhancement technique. Wavelet enhancements would provide different information to the low-vision observer and could prove to be superior to other enhancement techniques for some patients.

### *5.3 Recommendations for Follow-On Research*

The most obvious area that was not developed in this research was actual testing of the wavelet enhancement techniques. The steps necessary to do this would include:

- Measure the output of the headset with a photometer and develop a curve so that the non-linearity of the screens can be accounted for.
- Develop a digital to analog conversion scheme so that the output displays of the headset do not display Mach bands at the very low (threshold) contrast.
- Test visually impaired subjects for contrast sensitivity and contrast suprathreshold characteristics.
- Incorporate the suprathreshold contrast enhancement scheme outlined here with both Fourier techniques and wavelet techniques.
- Develop software to take advantage of the oculometer which tracks retinal movement so that just the area of the retina in the subject receives an enhanced image segment.
- Test wavelet enhancement schemes using bi-orthogonal wavelets as well as other symmetric wavelets.

## Appendix A. Peli Simulation

The simulation of what a person with a give contrast threshold sees was accomplished with the m-file scotoma.m:

```
%This function will simulate what a person with central scotoma sees (outputimage) when looking at a picture (inputimage).
function outputimage=scotoma(inputimage, threshold)
[m,n]=size(inputimage);
inputimage=real(inputimage);
for i=1:m;
for j=1:n;
if real(inputimage(i,j))>255;
inputimage(i,j)=255;
elseif real(inputimage(i,j))<0;
inputimage(i,j)=0;
end
end
end

F=fftshift(fft2(fftshift(inputimage)));
load log_cos

A0=F.*G0;
A1=F.*G1;
A2=F.*G2;
A3=F.*G3;
A4=F.*G4;
A5=F.*G5;

a1=(fftshift(ifft2(fftshift(A1))));
a2=(fftshift(ifft2(fftshift(A2))));
a3=(fftshift(ifft2(fftshift(A3))));
a4=(fftshift(ifft2(fftshift(A4))));
a5=(fftshift(ifft2(fftshift(A5))));

L1=A0;
L1=(fftshift(ifft2(fftshift(L1))));

L2=A1+L1;
L2=(fftshift(ifft2(fftshift(L2))));

L3=A2+L2;
L3=(fftshift(ifft2(fftshift(L3))));

L4=A3+L3;
L4=(fftshift(ifft2(fftshift(L4))));

L5=A4+L4;
L5=(fftshift(ifft2(fftshift(L5))));

c1=(a1)./l1;
c2=(a2)./l2;
c3=(a3)./l3;
c4=(a4)./l4;
c5=(a5)./l5;

for u=1:m;
for v=1:n;
if abs(c1(u,v))<=threshold(1);
final1(u,v)=0;
else;
final1(u,v)=(a1(u,v));
end;

if abs(c2(u,v))<=threshold(2);
final2(u,v)=0;
else;
final2(u,v)=(a2(u,v));
end;
```

```
if abs(c3(u,v))<=threshold(3);
final3(u,v)=0;
else;
final3(u,v)=(a3(u,v));
end;

if abs(c4(u,v))<=threshold(4);
final4(u,v)=0;
else;
final4(u,v)=(a4(u,v));
end;

if abs(c5(u,v))<=threshold(5);
final5(u,v)=0;
else;
final5(u,v)=(a5(u,v));
end;
end

outputimage=(11+final1+final2+final3+final4+final5);
```

## Appendix B. Enhancement Algorithms

This appendix contains the code used for the various not-wavelet enhancement algorithms outlined in this thesis.

```
function newpicture=adap_filter(picture)
picture=pad2(picture,zeros(21));
[A,B]=size(picture);
lowpass=zeros(A,B);
inverse=1/(21^2);
for x=11:(A-11)
for y=11:(B-11)
lowpass(x,y)=sum(sum(picture(x-10:x+10,y-10:y+10)))*inverse;
end
end
highpass=5*(picture-lowpass);

for x=1:A-20
for y=1:B-20
lowpass2(x,y)=lowpass(x+10,y+10);
highpass2(x,y)=highpass(x+10,y+10);
end
end
newpicture=highpass2+lowpass2;

%This function will apply the pre-emphasis filter to the inputimage.
function outputimage=emphasis(inputimage)
[m,n]=size(inputimage);
inputimage=real(inputimage);
for i=1:m;
for j=1:n;
if real(inputimage(i,j))>255;
inputimage(i,j)=255;
elseif real(inputimage(i,j))<0;
inputimage(i,j)=0;
end
end
F=fftshift(fft2(fftshift(inputimage)));
load log_cos
A0=F.*G0;
A1=F.*G1;
A2=F.*G2;
A3=F.*G3;
A4=F.*G4;
A5=F.*G5;
a4=5*(fftshift(ifft2(fftshift(A4))));
L1=A0;
L1=(fftshift(ifft2(fftshift(L1))));
L2=A1+L1;
L2=(fftshift(ifft2(fftshift(L2))));
L3=A2+L2;
L3=(fftshift(ifft2(fftshift(L3))));
L4=A3+L3;
L4=(fftshift(ifft2(fftshift(L4))));
outputimage=(a4+L4);
outputimage=heq(outputimage,255);
```

## *Appendix C. Matlab Implementation of Biorthogonal Wavelets*

### *C.1 Coefficients*

To decompose an image, a scaling function and a wavelet function are needed. With the biorthogonal wavelets used in this thesis, the scaling function and wavelet function for decomposition were defined in the file FBI.m as:

```
scaletilde=[0 .037828455506995 -.023849465019380...
-.11062440441842 .37740285561265 .85269867900940...
.37740285561265 -.11062440441842 -.023849465019380...
.037828455506995 0];

waveletilde=[0 0 0 .065438882628938 -.040689417609558...
-.41809227322221 .78858561640566 -.41809227322221...
-.040689417609558 .065438882628938 0];
```

The waveforms generated and their relationship are shown in figure 27. The extra zeros in the definitions are for Matlab purposes, since convolution was used. In addition to the code shown above, the following was also in the file FBI.m:

```
L=length(scaletilde);
for n=2:L-1;
wavelet(n-1)=((-1)^(n))*scaletilde(L-n+1);
end

wavelet(L-1)=((-1)^n)*scaletilde(L-n);
wavelet(L)=((-1)^n)*scaletilde(L-n);

L=length(wavelet);
for n=1:L-1;
scale(n+1)=((-1)^(n-1))*waveletilde(L-n+1);
end

scale(1)=((-1)^n)*waveletilde(L-n);
```

When executed in Matlab, the values in the vectors wavelet and scale were then:

```
wavelet =
Columns 1 through 7
```

0.0378 0.0238 -0.1106 -0.3774 0.8527 -0.3774 -0.1106

Columns 8 through 11

0.0238 0.0378 0 0

scale =

Columns 1 through 7

0 0 -0.0654 -0.0407 0.4181 0.7886 0.4181

Columns 8 through 11

-0.0407 -0.0654 0 0

These vectors and their relationship are shown in figure 31. Once again, the added zeros are due to Matlab implementation.

### C.2 Decomposition

With suitable coefficients, decomposition was a matter of careful implementation of the procedure outlined by Mallat (18) and Laing (14).

In the file Down2.m was the function Down2(inputface, level). The entire function code was:

```
%%%%%%%%%%%%%%%%%%%%%%%%%%%%%%%%%%%%%
%This m-file will decompose a two dimensional image according to %
% Mallat's method on page 685 of his 1979 wavelet paper, %
% corrected by Laing, with inputs from Maj. Greg Warhola. %
%%%%%%%%%%%%%%%%%%%%%%%%%%%%%%%%%%%%%
%%%%% Variables %%%%%%
%
%
% FACE.....image to be decomposed %
% face.....dummy variable so FACE will not be affected %
% LEVEL.....how many LEVELS user wishes to decompose %
% set.....which wavelet set to use %
% taps.....how many Daubechies taps to use %
% scaletilde.....low frequency impulse response used for decomposition %
% wavelettilde.....high frequency impulse response used for decomposition %
% L,K.....size of image at any given decomposition level %
% decompose_level.....current level of decomposition %
% gface.....face convolved with the column vector wavelettilde' %
% hface.....face convolved with the column vector scaletilde' %
% gfacedown.....downsampled gface (every other row, size L/2 x K) %
% hfacedown.....downsampled hface (every other row, size L/2 x K) %
```

```

% gface.....gface down convolved with row vector wavelettilde %
% hgface.....hfacedown convolved with row vector wavelettilde %
% ghface.....gfacedown convolved with row vector scaletilde %
% hhface.....hfacedown convolved with row vector scaletilde %
% D1_.....downsampled gface (every other column, size L/2 x K/2) %
% D2_.....downsampled hgface (every other column, size L/2 x K/2) %
% DL_.....downsampled ghface (every other column, size L/2 x K/2) %
% A_.....downsampled hhface (every other column, size L/2 x K/2) %
% LEVEL_.....name of file containing D1_, D2_, DL_, and A_F %

%%%%%
function Down2(FACE,LEVEL);

%%%%%
% This line would let a specific wavelet set be used. For this research,
% the FBI set was used for enhancement.
%
%x=input('Wavelet set to use: 1)Mallat 2)FBI 3)Battle 4)Daubechies...');
x=2;
y=20;
save which x

if x==1
Mallat;
M=length(scaletilde);
middle=ceil(M/2);
elseif x==2
FBI;
M=length(scaletilde);
middle=ceil(M/2);
elseif x==3
Battle;
M=length(scaletilde);
middle=ceil(M/2);
elseif x==4
% y=input('How many taps? Enter: 4 6 8 10 12 14 16 18 20...');
save whether y
Daubs;
M=length(scaletilde);
middle=ceil(M/2);
end
%%%%%
%
% The mirrorface function causes FACE to be quadrupled to minimize edge effects. The
% original image matrix can be thought of as quadrant one, quadrant two is the mirror
% image of quadrant one while quadrants three and four are the mirror image of quadrants
% one and two. This causes the image to be 2*L x 2*K in size.
%
%%%%%
face=mirrorface(FACE);
if face==FACE;
[L,K]=size(face);
M=length(scaletilde);

middle=ceil(M/2);

decompose_level=1;
while decompose_level<=LEVEL
decompose_level;

clear hface gface
for k=1:K;
for l=1:L;
hface(l,k)=0;
gface(l,k)=0;
for m=1:M;
%%%%%
%
% arg is a virtual argument for circular convolution. The following
% insures circular convolution occurs regardless of the size of the
% current matrix
%
%%%%%
arg=l-m+middle;
while (arg>L)|(arg<=0)
if arg>L
arg=arg-L;
elseif arg<=0
arg=L+arg;
end
end
%%%%%
%
% The following is the actual filtering of the scale and wavelet
% functions in the direction of decomposition
%

```

```

#####
hface(1,k)=hface(1,k)+face(arg,k)*scaletilde(m);
gface(1,k)=gface(1,k)+face(arg,k)*wavelettilde(m);
end
end
end

clear gfacdown hfacedown ggface hgface ghface hhface
#####
%
% Downsampling the columns
%
#####
for l=1:L/2;
gfacdown(l,:)=gface(2*l,:);
hfacedown(l,:)=hface(2*l,:);
end

for l=1:L/2;
for k=1:K;
ggface(L/2,K)=0;
hgface(L/2,K)=0;
ghface(L/2,K)=0;
hhface(L/2,K)=0;

for m=1:M;
#####
%
% arg is a virtual argument for circular convolution. The following
% insures circular convolution occurs regardless of the size of the
% current matrix
%
#####
arg=k-m+middle;
while (arg>K)|(arg<=0)
if arg>K
arg=arg-K;
elseif arg<=0
arg=K+arg;
end
end
#####
%
% The following is the actual filtering with the scale and wavelet
% functions in the direction of decomposition
%
#####
hhface(l,k)=hhface(l,k)+hfacedown(l,arg)*scaletilde(m);
ghface(l,k)=ghface(l,k)+gfacdown(l,arg)*scaletilde(m);
hgface(l,k)=hgface(l,k)+hfacedown(l,arg)*wavelettilde(m);
ggface(l,k)=ggface(l,k)+gfacdown(l,arg)*wavelettilde(m);
end
end
end

#####
%
% Downsampling the rows
%
#####
for k=1:K/2;
eval(['D1_-' int2str(decompose_level) '(:,k)=ggface(:,2*k)']);
eval(['D2_-' int2str(decompose_level) '(:,k)=hgface(:,2*k)']);
eval(['D1_-' int2str(decompose_level) '(:,k)=hgface(:,2*k)']);
eval(['A_-' int2str(decompose_level) '(:,k)=hhface(:,2*k)']);
end

#####
%
% Saving the current decomposition level coefficients
%
#####
eval(['save LEVEL_' int2str(decompose_level) ' D1_-' int2str(decompose_level) ...
'D2_-' int2str(decompose_level) ' D1_-' int2str(decompose_level) ' A_-' ...
int2str(decompose_level)]);
eval(['face=A_-' int2str(decompose_level) ';'])
L=L/2;
K=K/2;
decompose_level=decompose_level+1;
end

```

### C.3 Reconstruction

The reconstruction code was in the file Up2.m and was:

```

%%%%%%%%%%%%%%%%%%%%%%%%%%%%%%%%%%%%% Variables %%%%%%
%
% LEVEL..... how many LEVELs were decomposed %
% set..... which wavelet set was used %
% taps..... how many Daubechies taps were used %
% scale..... low frequency impulse response used for decomposition %
% wavelet..... high frequency impulse response used for decomposition %
% A..... current image matrix to be upsampled and convolved %
% L,K..... size of image at any given reconstruction level %
% reconstruct_level..... current level of decomposition %
% LEVEL_..... name of file containing D3_, D2_, D1_, and A_ %
% D3_..... diagonal detail coefficients at current level %
% D2_..... horizontal detail coefficients at current level %
% D1_..... vertical detail coefficients at current level %
% A_..... approximation coefficients at current level %
% gfacetemp..... D3_ with rows upsampled and zero padded (size L x 2*k) %
% hgfacetemp..... D2_ with rows upsampled and zero padded (size L x 2*k) %
% ghfacetemp..... D1_ with rows upsampled and zero padded (size L x 2*k) %
% hhfacetemp..... A with rows upsampled and zero padded (size L x 2*k) %
% ggface..... gfacetemp convolved with the row vector wavelet %
% hgface..... hgfacetemp convolved with the row vector scale %
% ghface..... ghfacetemp convolved with the row vector wavelet %
% hhface..... hhfacetemp convolved with the row vector scale %
% gfacedown..... ggface+hgface %
% hfacedown..... hgface+hhface %
% gfacetemp..... gfacedown, cols upsampled (size 2*L x 2*k) %
% hfacetemp..... hfacedown, cols upsampled (size 2*L x 2*k) %
% gface..... gfacetemp convolved with the column vector wavelet' %
% hface..... hfacetemp convolved with the column vector scale' %
% face..... resulting reconstructed image %

function face=Up2(LEVEL);

% For this research, x=2 was used for the FBI wavelet set.
%

load which

if x==1
Mallat;
gain=2;
M=length(scale);
middle=ceil(M/2);
elseif x==2
FBI;
gain=1;
M=length(scale);
middle=ceil(M/2);
elseif x==3
Battle;
gain=1;
M=length(scale);
middle=ceil(M/2);
elseif x==4
load whether
Daubs;
gain=1;
M=length(scale);
middle=ceil(M/2);
end

reconstruct_level=LEVEL;
while reconstruct_level>0
reconstruct_level;

eval(['load LEVEL_ ' int2str(reconstruct_level)])>

if reconstruct_level==LEVEL
eval(['A=A_ ' int2str(reconstruct_level) ';'])
else

```

```

A=face;
end

M=length(scale);
[L,K]=size(A);
L=2*L;
K=2*K;

middle=ceil(M/2);
ends=floor(M/2);

ggfacetemp=zeros(L/2,K);
hgfacetemp=zeros(L/2,K);
ghfacetemp=zeros(L/2,K);
hhfacetemp=zeros(L/2,K);

#####
% Upsampling the rows
% #####
for k=1:K/2;
eval(['ggfacetemp(:,2*k)=D3_'' int2str(reconstruct_level) '(:,k);']);
eval(['hgfacetemp(:,2*k)=D2_'' int2str(reconstruct_level) '(:,k);']);
eval(['ghfacetemp(:,2*k)=D1_'' int2str(reconstruct_level) '(:,k);']);
hhfacetemp(:,2*k)=A(:,k);
end

for l=1:L/2;
for k=1:K;
ggface(l,k)=0;
hgface(l,k)=0;
ghface(l,k)=0;
hhface(l,k)=0;

for m=1:M;
#####
% arg is a virtual argument for circular convolution. The following
% insures circular convolution occurs regardless of the size of the
% current matrix
%
arg=k+m+middle;
while (arg>K)|(arg<=0)
if arg>K
arg=arg-K;
elseif arg<=0
arg=K+arg;
end
end
#####
% The following is the actual filtering of the scale and wavelet
% functions in the direction of decomposition
%
ggface(l,k)=ggface(l,k)+ggfacetemp(l,arg)*wavelet(m);
hgface(l,k)=hgface(l,k)+hgfacetemp(l,arg)*scale(m);
ghface(l,k)=ghface(l,k)+ghfacetemp(l,arg)*wavelet(m);
hhface(l,k)=hhface(l,k)+hhfacetemp(l,arg)*scale(m);
end
end
end

gfacedown=ggface+hgface;
hfacedown=ghface+hhface;

clear gfacetemp hfacetemp gface hface

gfacetemp=zeros(L,K);
hfacetemp=zeros(L,K);

#####
% Upsampling the columns
%
#####
for l=1:L/2;
gfacetemp(2*l,:)=gfacedown(l,:);
hfacetemp(2*l,:)=hfacedown(l,:);
end

clear hface gface
for k=1:K;
for l=1:L;

```

```

hface(l,k)=0;
gface(l,k)=0;
for m=1:M;
%%%%%
%
% arg is a virtual argument for circular convolution. The following
% insures circular convolution occurs regardless of the size of the
% current matrix
%
%%%%%
arg1=m+middle;
while (arg>L)|(arg<0)
if arg>L
arg=arg-L;
elseif arg<0
arg=L+arg;
end
end
%
% The following is the actual filtering with the scale and wavelet
% functions in the direction of decomposition
%
%%%%%
hface(l,k)=hface(l,k)+gfacetemp(arg,k)*wavelet(m);
gface(l,k)=gface(l,k)+hfacetemp(arg,k)*scale(m);
end
end
end
face=(gface+hface)*gain;
reconstruct_level=reconstruct_level-1;
end
%%%%%
%
% This step ensures an image the same size as the original. (Remember,
% the mirrorimage function was used to minimize edge effects)
%
%%%%%
face=(face(1:L/2,1:K/2)+face(L:-1:L/2+1,1:K/2)+face(1:L/2,K:-1:K/2+1)+face(L:-1:L/2+1,K:-1:K/2+1))/4;

return

```

## Appendix D. Wavelet Simulation Code

The Matlab code in this appendix explains how the simulation of visual perception based on contrast sensitivity using bi-orthogonal wavelets was implemented.

```

%%%%%%%%%%%%%%%%%%%%%%%%%%%%%%%%%%%%%
% This function will create a contrast image at each level corresponding to
% measured points on the contrast threshold curve, and then use that data to
% manipulate the detail coefficients at each level. The returned image, waveface
% will be a wavelet simulation of what a person with a given contrast threshold
% sees when looking at the original image, FACE.
%
%
%%%%%%%%%%%%%%%%%%%%%%%%%%%%%%%%%%%%%
%           VARIABLES           %
%
% FACE..... input image
% face..... dummy variable so FACE will not be changed
% threshold, t ..... contrast threshold used for given person
% LEVEL..... maximum level of decomposition, image size dependant
% L,K..... size of face
% LEVEL_..... set of coefficients at current decomposition level
% D3_..... diagonal details
% D2_..... horizontal details
% D1_..... vertical details
% A..... approximation image at that level
% C, dummy..... contrast image at that level
%
%%%%%%%%%%%%%%%%%%%%%%%%%%%%%%%%%%%%%
function waveface=scotowave(FACE,threshold,scoLEVEL);

face=FACE;
t=threshold;

[L,K]=size(face);
for l=1:L;
for k=1:K;
if real(face(l,k))>255;
face(l,k)=255;
elseif real(face(l,k))<0;
face(l,k)=0;
end
end
end

Down2scowave(face,t,scoLEVEL);

waveface=Up2scowave(scoLEVEL);

%%%%%%%%%%%%%%%%%%%%%%%%%%%%%%%%%%%%%
%This m-file will decompose a two dimensional image according to
%Mallat's method on page 685 of his 1979 wavelet paper,
%corrected by Laing, with inputs from Maj. Greg Wazhola.
%
%%%%%%%%%%%%%%%%%%%%%%%%%%%%%%%%%%%%%
%           Variables           %
%
% FACE..... image to be decomposed
% face..... dummy variable so FACE will not be affected
% scoLEVEL..... how many LEVELs user wishes to decompose
% set..... which wavelet set to use
% taps..... how many Daubechies taps to use
% scaletilde..... low frequency impulse response used for decomposition
% scowavelettilde..... high frequency impulse response used for decomposition
% L,K..... size of image at any given decomposition level
% decompose_level..... current level of decomposition
% gface..... face convolved with the column vector scowavelettilde'
% hface..... face convolved with the column vector scaletilde'
% gfacedown..... downsampled gface (every other row, size L/2 x K)
% hfacedown..... downsampled hface (every other row, size L/2 x K)
% ggface..... gfacedown convolved with row vector scowavelettilde
% hgface..... hfacedown convolved with row vector scaletilde
% ghface..... gfacedown convolved with row vector scaletilde
%
```

```

% hhface.....hfacetdown convolved with row vector scaletilde %
% D3_ .....downsampled ggface (every other column, size L/2 x K/2) %
% D2_ .....downsampled ghface (every other column, size L/2 x K/2) %
% D1_ .....downsampled hgface (every other column, size L/2 x K/2) %
% A .....downsampled hhface (every other column, size L/2 x K/2) %
% scoLEVEL_ .....name of file containing scoD3_, scoD2_, scoD1_, and scoA_
%
%%%%%%%
function Down2scowave(FACE, threshold, scoLEVEL);

%%%%%%
% This line would let a specific wavelet set be used. For this research,
% the FBI set was used for simulation.
%
%x=input('Wavelet set to use: 1)Mallat 2)FBI 3)Battle 4)Daubechies...');
x=3;
ty=20;
save which x

if x==1
Mallat;
M=length(scaletilde);
middle=ceil(M/2);
elseif x==2
FBI;
M=length(scaletilde);
middle=ceil(M/2);
elseif x==3
Battle;
M=length(scaletilde);
middle=ceil(M/2);
elseif x==4
% y=input('How many taps? Enter: 4 6 8 10 12 14 16 18 20...');
save whether y
Daubs;
M=length(scaletilde);
middle=ceil(M/2);
end
%%%%%%
%
% The mirrorface function causes FACE to be quadrupled to minimize edge effects. The
% original image matrix can be thought of as quadrant one, quadrant two is the mirror
% image of quadrant one while quadrants three and four are the mirror image of quadrants
% one and two. This causes the image to be 2*L x 2*K in size.
%
%%%%%%

[L,K]=size(FACE);

face=mirrorface(FACE);

[L,K]=size(face);

M=length(scaletilde);

middle=ceil(M/2);

decompose_level=1;
while decompose_level<=scoLEVEL

clear hface gface ggface hgface ghface hhface

i=scoLEVEL-decompose_level-1;

cpi=(2^f)+(2^(i-1));

if cpi > 32
for k=1:K;
for l=1:L;
hface(l,k)=0;
for m=1:M;
%%%%%%
%
% arg is a virtual argument for circular convolution. The following
% insures circular convolution occurs regardless of the size of the
% current matrix
%
arg=l+middle;
while (arg>L)|(arg<=0)
if arg>L
arg=arg-L;
elseif arg<=0
arg=L+arg;
end
end
end

```

```

#####
#
# The following is the actual filtering of the scale and wavelet
# functions in the direction of decomposition
#
#####
hface(1,k)=hface(1,k)+face(arg,k)*scaletilde(m);

end
end
end
else
for k=1:K;
for l=1:L;
hface(l,k)=0;
gface(l,k)=0;
for m=1:M;
#####
#
# arg is a virtual argument for circular convolution. The following
# insures circular convolution occurs regardless of the size of the
# current matrix
#
#####
arg=1-m+middle;
while (arg>L)|(arg<=0)
if arg>L
arg=arg-L;
elseif arg<=0
arg=L+arg;
end
end
#####
#
# The following is the actual filtering of the scale and wavelet
# functions in the direction of decomposition
#
#####
hface(1,k)=hface(1,k)+face(arg,k)*scaletilde(m);
gface(1,k)=gface(1,k)+face(arg,k)*scowavelettilde(m);
end
end
end
if cpi > 32
for l=1:L;
for k=1:K;
hhface(l,k)=0;

for m=1:M;
#####
#
# arg is a virtual argument for circular convolution. The following
# insures circular convolution occurs regardless of the size of the
# current matrix
#
#####
arg=k-m+middle;
while (arg>K)|(arg<=0)
if arg>K
arg=arg-K;
elseif arg<=0
arg=K+arg;
end
end
#####
#
# The following is the actual filtering with the scale
# functions in the direction of decomposition
#
#####
hhface(l,k)=hhface(l,k)+hface(l,arg)*scaletilde(m);
end
end
end
else
for l=1:L;
for k=1:K;
ggface(l,k)=0;
hgface(l,k)=0;
ghface(l,k)=0;
hhface(l,k)=0;

for m=1:M;
#####
#
# arg is a virtual argument for circular convolution. The following

```

```

% insures circular convolution occurs regardless of the size of the
% current matrix
%
%%%%%%%%%%%%%
arg=k-m+middle;
while (arg>K)|(arg<0)
if arg>K
arg=arg-K;
elseif arg<0
arg=K+arg;
end
end
%
% The following is the actual filtering with the scale and wavelet
% functions in the direction of decomposition
%
%%%%%%%%%%%%%
ghface(1,k)=ghface(1,k)+gface(1,arg)*scaletilde(m);
hgface(1,k)=hgface(1,k)+hface(1,arg)*scowavelettilde(m);
ggface(1,k)=ggface(1,k)+gface(1,arg)*scowavelettilde(m);
hhface(1,k)=hhface(1,k)+hface(1,arg)*scaletilde(m);
end
end
end
end
if cpi < 32
Cgh=abs(ghface./(hhface+.00000001));
Chg=abs(hgface./(hhface+.00000001));
Cgg=abs(ggface./(hhface+.00000001));
[LC,KC]=size(Cgh);
for l=1:LC;
for k=1:KC;
if(Cgh(l,k) <= threshold(cpi))
ghface(l,k)=0;
end
if(Chg(l,k) <= threshold(cpi))
hgface(l,k)=0;
end
if(Cgg(l,k) <= threshold(cpi))
ggface(l,k)=0;
end
end
end
end
%
% Downsampling the rows and columns
%
%%%%%%%%%%%%%
if cpi < 32
for l=1:L/2;
for k=1:K/2;
if (2*l+1<=L) & (2*k+1<=K)
eval(['scod3_ ' int2str(decompose_level) '(l,k)=ggface(2*l+1,2*k+1);'])
eval(['scod2_ ' int2str(decompose_level) '(l,k)=ghface(2*l+1,2*k);'])
eval(['scod1_ ' int2str(decompose_level) '(l,k)=hgface(2*l,2*k+1);'])
eval(['scoA_ ' int2str(decompose_level) '(l,k)=hhface(2*l,2*k);'])
elseif (2*l+1>L) & (2*k+1<=K)
eval(['scod3_ ' int2str(decompose_level) '(l,k)=ggface(2*l+1,1);'])
eval(['scod2_ ' int2str(decompose_level) '(l,k)=ghface(2*l+1,2*k);'])
eval(['scod1_ ' int2str(decompose_level) '(l,k)=hgface(2*l,1);'])
eval(['scoA_ ' int2str(decompose_level) '(l,k)=hhface(2*l,2*k);'])
elseif (2*l+1>L) & (2*k+1>K)
eval(['scod3_ ' int2str(decompose_level) '(l,k)=ggface(1,2*k+1);'])
eval(['scod2_ ' int2str(decompose_level) '(l,k)=ghface(1,2*k);'])
eval(['scod1_ ' int2str(decompose_level) '(l,k)=hgface(2*l,2*k+1);'])
eval(['scoA_ ' int2str(decompose_level) '(l,k)=hhface(2*l,2*k);'])
else
eval(['scod3_ ' int2str(decompose_level) '(l,k)=ggface(1,1);'])
eval(['scod2_ ' int2str(decompose_level) '(l,k)=ghface(1,2*k);'])
eval(['scod1_ ' int2str(decompose_level) '(l,k)=hgface(2*l,1);'])
eval(['scoA_ ' int2str(decompose_level) '(l,k)=hhface(2*l,2*k);'])
end
end
end
else
eval(['scod3_ ' int2str(decompose_level) '=zeros(L/2,K/2);'])
eval(['scod2_ ' int2str(decompose_level) '=zeros(L/2,K/2);'])
eval(['scod1_ ' int2str(decompose_level) '=zeros(L/2,K/2);'])
for l=1:L/2;
for k=1:K/2;
eval(['scoA_ ' int2str(decompose_level) '(l,k)=hhface(2*l,2*k);'])
end
end
end

```

```

#####
#
# Saving the current decomposition level coefficients
#
#####
eval(['save scoLEVEL_ int2str(decompose_level) ' scoD3_ ' int2str(decompose_level) ...
'scoD2_ ' int2str(decompose_level) ' scoD1_ ' int2str(decompose_level) ' scoA_ ' ...
int2str(decompose_level)])]

eval(['face-scoA_ ' int2str(decompose_level) ';''])

L=L/2;
K=K/2;
decompose_level=decompose_level+1;

end

#####
#
#This m-file will reconstruct a two dimensional image according to
#Mallat's method on page 685 of his 1979 wavelet paper,
#corrected by Laing, with inputs from Maj. Greg Warhola.
#
#####

Variables
#####
%
%
% scoLEVEL.....how many LEVELS were decomposed %
% set.....which wavelet set was used %
% taps.....how many Daubechies taps were used %
% scale.....low frequency impulse response used for decomposition %
% wavelet.....high frequency impulse response used for decomposition %
% A.....current image matrix to be upsampled and convolved %
% L,K.....size of image at any given reconstruction level %
% reconstruct_level.....current level of decomposition %
% scoLEVEL.....name of file containing D3_, D2_, D1_, and A_
% D3_.....diagonal detail coefficients at current level %
% D2_.....horizontal detail coefficients at current level %
% D1_.....vertical detail coefficients at current level %
% A_.....approximation coefficients at current level %
% ggfacetemp.....D3_ with rows upsampled and zero padded (size L x 2*k) %
% hgfacetemp.....D2_ with rows upsampled and zero padded (size L x 2*k) %
% ghfacetemp.....D1_ with rows upsampled and zero padded (size L x 2*k) %
% hhfacetemp.....A with rows upsampled and zero padded (size L x 2*k) %
% ggface.....ggfasetemp convolved with the row vector wavelet %
% hface.....hgfasetemp convolved with the row vector scale %
% ghface.....ghfasetemp convolved with the row vector wavelet %
% hhface.....hhfasetemp convolved with the row vector scale %
% gfacetemp.....ggface+hhface %
% hfacedown.....gface %
% gfacedown.....gface+hhface %
% gfacetemp.....gfacedown, cols upsampled (size 2*L x 2*k) %
% hfacedown.....hfacedown, cols upsampled (size 2*L x 2*k) %
% gface.....gfacetemp convolved with the column vector wavelet %
% hface.....hfacetemp convolved with the column vector scale %
% face.....resulting reconstructed image %

function face=Up2sacwave(scoLEVEL);
#####
#
# For this research, x=2 was used for the FBI wavelet set.
#
%

load which

if x==1
Mallat;
gain=2;
M=length(scale);
middle=ceil(M/2);
elseif x==2
FBI;
gain=1;
M=length(scale);
middle=ceil(M/2);
elseif x==3
Battle;
gain=1;
M=length(scale);
middle=ceil(M/2);
elseif x==4
load whether
Daubs;
gain=1;
M=length(scale);
middle=ceil(M/2);
end

```

```

reconstruct_level=scoLEVEL;
while reconstruct_level>0

clear hface gface ggface hgface ghface hhface

eval(['load scoLEVEL_` int2str(reconstruct_level)'])

if reconstruct_level==scoLEVEL
eval(['A=scoA_` int2str(reconstruct_level) `'])
else
A=face;
end

M=length(scale);
[L,K]=size(A);
L=2*L;
K=2*K;

middle=ceil(M/2);
ends=floor(M/2);

ggfacetemp=zeros(L/2,K);
hgfacetemp=zeros(L/2,K);
ghfacetemp=zeros(L/2,K);
hhfacetemp=zeros(L/2,K);

#####
% Upsampling the rows
#####

size(ggfacetemp);
eval(['size(scoD3_` int2str(reconstruct_level) `)']);
for k=1:K/2;
eval(['ggfacetemp(:,2*k)=scoD3_` int2str(reconstruct_level) `(:,k);']);
eval(['hgfacetemp(:,2*k)=scoD2_` int2str(reconstruct_level) `(:,k);']);
eval(['ghfacetemp(:,2*k)=scoD1_` int2str(reconstruct_level) `(:,k);']);
hhfacetemp(:,2*k)=A(:,k);
end

for l=1:L/2;
for k=1:K;
ggface(l,k)=0;
hgface(l,k)=0;
ghface(l,k)=0;
hhface(l,k)=0;

for m=1:M;
#####
% arg is a virtual argument for circular convolution. The following
% insures circular convolution occurs regardless of the size of the
% current matrix
%
#####
arg=k-m+middle;
while (arg>K)|(arg<=0)
if arg>K
arg=arg-K;
elseif arg<=0
arg=K+arg;
end
end
#####
% The following is the actual filtering of the scale and wavelet
% functions in the direction of decomposition
%
#####
ggface(l,k)=ggface(l,k)+ggfacetemp(l,arg)*wavelet(m);
hgface(l,k)=hgface(l,k)+hgfacetemp(l,arg)*scale(m);
ghface(l,k)=ghface(l,k)+ghfacetemp(l,arg)*wavelet(m);
hhface(l,k)=hhface(l,k)+hhfacetemp(l,arg)*scale(m);
end
end
end

gfacedown=ggface+hgface;
hfacedown=ghface+hhface;

clear gfacetemp hfacetemp gface hface

gfacetemp=zeros(L,K);
hfacetemp=zeros(L,K);

```

```

#####
#
# Upsampling the columns
#
#####

for l=1:L/2;
gfacetemp(2*l,:)=gfacedown(l,:);
hfacetemp(2*l,:)=hfacedown(l,:);
end

clear hface gface
for k=1:L;
for l=1:L;
hface(l,k)=0;
gface(l,k)=0;
for m=1:M;
#####
#
# arg is a virtual argument for circular convolution. The following
# insures circular convolution occurs regardless of the size of the
# current matrix
#
#####
arg=l-m+middle;
while (arg>L)|(arg<=0)
if arg>L
arg=arg-L;
elseif arg<=0
arg=L+arg;
end
end
#####
#
# The following is the actual filtering with the scale and wavelet
# functions in the direction of decomposition
#
#####

hface(l,k)=hface(l,k)+gfacetemp(arg,k)*wavelet(m);
gface(l,k)=gface(l,k)+hfacetemp(arg,k)*scale(m);
end
end
end
face=(gface+hface)*gain;
reconstruct_level=reconstruct_level-1;
end
#####
#
# This step ensures an image the same size as the original. (Remember,
# the mirrorimage function was used to minimize edge effects)
#
#####

face=(face(1:L/2,1:K/2)+face(L:-1:L/2+1,1:K/2)+face(1:L/2,K:-1:K/2+1)+face(L:-1:L/2+1,K:-1:K/2+1))/4;

return

```

## Bibliography

1. Boyd, Robert W. *Radiometry and the Detection of Optical Radiation*. New York / Chinchester / Brisbane / Toronto / Singapore: John Wiley and Sons, 1983.
2. Cannon, Mark W. "Perceived Contrast in the Fovea and Periphery," *Journal of the Optical Society of America*, 2:1760-68 (October 1985).
3. Cannon, Mark W. and Steven C. Fullenkamp. "Perceived Contrast and Stimulus Size: Experiment and Simulation," *Vision Research*, 28(6):695-709 (1988).
4. Chang, Tianhorng and C.-C. Jay Kuo. "Texture Analysis and Classification with Tree-Structured Wavelet Transform," *IEEE Transactions on Image Processing*, 2(4):429-441 (October 1993).
5. Cohen, Albert and Ingrid Daubechies. "Wavelets on the Interval and Fast Wavelet Transforms," *Applied and Computational Harmonic Analysis*, 1:54-81 (1993).
6. Cornsweet, Tom N. "The Staircase-Method in Psychophysics," *The American Journal of Psychology*, 75:485-491 (1962).
7. Fine, Elisabeth M. and others. "Image Enhancement of Scrolled Text," *Technical Digest Series*, 2:254-257 (February 1994).
8. Ginsburg, Arthur P. *Visual Information Processing Based on Spatial Filters Constrained by Biological Data*. PhD Dissertation, University of Cambridge, December 1978.
9. Gonzalez, Rafael C. and Richard E. Woods. *Digital Image Processing* (Third Edition). New York: Addison-Wesley Publishing Company, 1992.
10. Hopper, Tom and others. "Compression of Grey-Scale Fingerprint Images," *IEEE: Proceedings from Data Compression Conference*, 309-318 (1992).
11. Interservice/Industry Training Systems Conference. *Design of an Eye Slaved Area of Interest System for the Simulator Complexity Testbed*, November 1989.
12. Jones, Judson P. and others. "The Two-Dimensional Spectral Structure of Simple Receptive Fields in Cat Striate Cortex," *Journal of Neurophysiology*, 58(6):1212-1232 (December 1987).
13. Jones, Judson P. and Larry A. Palmer. "An Evaluation of the Two-Dimensional Gabor Filter Model of Simple Receptive Fields in Cat Striate Cortex," *Journal of Neurophysiology*, 58(6):1233-1258 (December 1987).
14. Laing, Capt John S. *Analysis of Visual Illusions Using Multiresolution Wavelet Decomposition Based Models*. Masters Thesis, Graduate School of Engineering, Air Force Institute of Technology (AETC), Wright-Patterson AFB OH, December 1991.
15. Lawton, Teri B. "Improved Word Recognition for Observers with Age-Related Maculopathies Using Compensation Filters," *Opt Vision Sci*, 3(2):125-135 (1988).

16. Lieberman, Harris R. and Alex P. Pentland. "Microcomputer-Based Estimation of Psychophysical Thresholds: The Best PEST," *Behavior Research Methods & Instrumentation*, 14(1):21–25 (1982).
17. MacDonald, Robert P. *Optical Wavelet Transform for Fingerprint Identification*. Masters Thesis, Graduate School of Engineering, Air Force Institute of Technology (AETC), Wright-Patterson AFB OH, December 1993.
18. Mallat, Stephane G. "A Theory for Multiresolution Signal Decomposition: The Wavelet Representation," *IEEE Transactions on Pattern Analysis and Machine Intelligence*, 11(7):674–693 (July 1989).
19. Peli, Eli. "Contrast in Complex Images," *Optical Society of America*, 7(10):2032–2040 (October 1990).
20. Peli, Eli. "New Perspectives on Image Enhancement for the Visually Impaired," *SPIE*, 1382:49–59 (1990).
21. Peli, Eli. "Limitations of Image Enhancement for the Visually Impaired," *Optometry and Vision Science*, 69(1):15–24 (December 1991).
22. Peli, Eli and others. "Computerized Image Enhancement for Visually Impaired Persons: New Technology, New Possibilities," *Journal of Visual Impairment and Blindness*, 849–854 (September 1986).
23. Peli, Eli and others. "Contrast Sensitivity Functions for Analysis and Simulation of Visual Perception," *Optical Society of America*, 3:126–129 (February 1990). Noninvasive Assessment of the Visual System 1990 Technical Digest Series.
24. Peli, Eli and others. "Image Enhancement for the Visually Impaired," *Investigative Ophthalmology and Visual Science*, 32(8):2337–2350 (July 1991).
25. Peli, Eli and others. "Image Invariance with Changes in Size: the Role of Peripheral Contrast Thresholds," *Optical Society of America*, 8(11):1762–1774 (November 1991).
26. Peli, Eli and Tamar Peli. "Image Enhancement for the Visually Impaired," *Optical Engineering*, 23(1):047–051 (January/February 1984).
27. Peli, Tamar and Jae S. Lim. "Adaptive Filtering for Image Enhancement," *Optical Engineering*, 21(1):108–112 (January 1982).
28. Pentland, Alex. "Maximum Likelihood Estimation: The Best PEST," *Perception & Psychophysics*, 28(4):377–379 (1980).
29. Rioul, Olivier and Martin Vetterli. "Wavelets and Signal Processing," *IEEE SP Magazine*, 14–38 (1991).
30. Rothenberg, Mikel A. and Charles F. Chapman. *Dictionary of Medical Terms for the Nonmedical Person*. Barron's, 1989.

31. Rubin, Gary S. and Ronald A. Schuchard. "Does Contrast Sensitivity Predict Face Recognition Performance in Low-Vision Observers," *Optical Society of America*, 3:130–133 (February 1990). Noninvasive Assessment of the Visual System 1990 Technical Digest Series.
32. Stockham, Thomas G. "Image Processing in the Context of a Visual Model," *Proceedings of the IEEE*, 60(7):828–842 (July 1972).
33. Taylor, M. M. and C Douglas Creelman. "PEST: Efficient Estimates on Probability Functions," *Journal of the Acoustical Society of America*, 41(4):782–787 (1967).
34. Wald, Abraham. *Sequential Analysis*. London: John Wiley & Sons, Inc., 1947.
35. Wang, Kuansan and Shihab A. Shamma. "Modeling the auditory functions in the primary cortex," *Optical Engineering*, 33(7):2143–2150 (July 1994).
36. Werblin, Frank S. "The Control of Sensitivity in the Retina," *Offprint: Scientific American*, 228(1):71–79 (January 1973).
37. Wickerhauser, Mladen Victor. "High-Resolution Still Picture Compression," *Digital Signal Processing*, 2:204–226 (1992).
38. Williams, T. and others, "Techniques and Methods Used in Eye-Tracking in the Fiber-optic Helmet-Mounted Display." Image IV conference, 1987.
39. Zeki. *A Vision of the Brain*. Blackwell Scientific Publications, 1994.

*Vita*

Capt Myers was born on Scott AFB, IL in 1965. After serving in the Missouri Air National Guard as a Radio Operator during his years at the University of Missouri-Rolla, he received a degree in Electrical Engineering and attended Officer Training School at Lackland AFB, TX in 1989. He attended Specialized Undergraduate Navigator Training at Mather AFB, CA and became a Defensive Systems Officer in the B-1B heavy bomber at Ellsworth AFB, SD. He graduated from the Air Force Institute of Technology with a Masters in Electrical Engineering from class GEO-94D in 1994.

Permanent address: 404 Redbud Ln.  
Dayton, OH 45433

# REPORT DOCUMENTATION PAGE

**Form Approved  
OMB No. 0704-0188**

Public reporting burden for this collection of information is estimated to average 1 hour per response, including the time for reviewing instructions, searching existing data sources, gathering and maintaining the data needed, and completing and reviewing the collection of information. Send comments regarding this burden estimate or any other aspect of this collection of information, including suggestions for reducing this burden, to Washington Headquarters Services, Directorate for Information Operations and Reports, 1215 Jefferson Davis Highway, Suite 1204, Arlington, VA 22202-4302, and to the Office of Management and Budget, Paperwork Reduction Project (0704-0188), Washington, DC 20503.

1. AGENCY USE ONLY (Leave blank)	2. REPORT DATE	3. REPORT TYPE AND DATES COVERED	
4. TITLE AND SUBTITLE	5. FUNDING NUMBERS		
Image Perception Wavelet Simulation and Enhancement for the Visually Impaired			
6. AUTHOR(S)			
Lemuel Ray Myers, Jr.			
7. PERFORMING ORGANIZATION NAME(S) AND ADDRESS(ES)		8. PERFORMING ORGANIZATION REPORT NUMBER	
Air Force Institute of Technology, WPAFB OH 45433-6583		AFIT/GEO/ENG/94D-03	
9. SPONSORING/MONITORING AGENCY NAME(S) AND ADDRESS(ES)		10. SPONSORING/MONITORING AGENCY REPORT NUMBER	
11. SUPPLEMENTARY NOTES			
12a. DISTRIBUTION/AVAILABILITY STATEMENT		12b. DISTRIBUTION CODE	
Distribution Unlimited			
13. ABSTRACT (Maximum 200 words)			
This research delves into the area of image enhancement for the visually impaired. Binocular macular degeneration, a visual impairment, affects many Americans; since this condition could not be corrected with conventional glasses, the literature suggested using an enhancement system which used a pre-emphasis algorithm to enhance the input image for output to the observer. The work of Dr. Eli Peli, a pioneer in the field of image enhancement, is examined and reproduced. Since his work concentrated mainly on frequency analysis of images, the bulk of this research involves using discrete wavelet analysis to augment that work. A biorthogonal wavelet set is used to enhance images. That same wavelet set is used to provide a simulation of a person's perception of an image based upon that person's contrast sensitivity function. The wavelet enhancement follows Dr. Peli's method of enhancement using a modified pre-emphasis filter. The wavelet enhancement results are similar to that technique, with the most notable difference being that wavelet enhancements tend to accentuate the horizontal and vertical details of the image more than the spatial frequency concentric filter techniques outlined by Peli and others. The perception simulations use wavelet analysis and are based on the work accomplished by Peli concerning "local band-limited contrast," with the frequency analysis of that work giving way to a wavelet analysis; the results here are significantly different than those results seen in the Peli simulation.			
14. SUBJECT TERMS		15. NUMBER OF PAGES 95	
Image Enhancement, Wavelet Simulation, Wavelet Analysis, Wavelet Enhancement		16. PRICE CODE	
17. SECURITY CLASSIFICATION OF REPORT  UNCLASSIFIED	18. SECURITY CLASSIFICATION OF THIS PAGE  UNCLASSIFIED	19. SECURITY CLASSIFICATION OF ABSTRACT  UNCLASSIFIED	20. LIMITATION OF ABSTRACT  UL